










Bispecific antibodies redirect synthetic agonistic receptor modified T cells against melanoma

Florian Märkl ¹, Mohamed-Reda Benmebarek ¹, Julius Keyl,¹ Bruno L Cadilha,¹ Martina Geiger,² Clara Karches,¹ Hannah Obeck,¹ Melanie Schwerdtfeger,¹ Stefanos Michaelides,¹ Daria Briukhovetska,¹ Sophia Stock ^{1,3,4}, Jakob Jobst,¹ Philipp Jie Müller,¹ Lina Majed,¹ Matthias Seifert ¹, Anna-Kristina Klüver,¹ Theo Lorenzini ¹, Ruth Grünmeier ¹, Moritz Thomas ^{5,6,7}, Adrian Gottschlich,¹ Richard Klaus,⁸ Carsten Marr,^{5,6} Michael von Bergwelt-Baildon,^{3,4} Simon Rothenfusser,¹ Mitchell P Levesque,⁹ Markus Vincent Heppt,^{10,11} Stefan Endres ^{1,4,12}, Christian Klein ², Sebastian Kobold ^{1,4,12}

To cite: Märkl F, Benmebarek M-R, Keyl J, et al. Bispecific antibodies redirect synthetic agonistic receptor modified T cells against melanoma. *Journal for ImmunoTherapy of Cancer* 2023;11:e006436. doi:10.1136/jitc-2022-006436

► Additional supplemental material is published online only. To view, please visit the journal online (<http://dx.doi.org/10.1136/jitc-2022-006436>).

FM and M-RB contributed equally.

Accepted 16 April 2023



© Author(s) (or their employer(s)) 2023. Re-use permitted under CC BY-NC. No commercial re-use. See rights and permissions. Published by BMJ.

For numbered affiliations see end of article.

Correspondence to

Professor Sebastian Kobold; sebastian.kobold@med.uni-muenchen.de

ABSTRACT

Background Melanoma is an immune sensitive disease, as demonstrated by the activity of immune check point blockade (ICB), but many patients will either not respond or relapse. More recently, tumor infiltrating lymphocyte (TIL) therapy has shown promising efficacy in melanoma treatment after ICB failure, indicating the potential of cellular therapies. However, TIL treatment comes with manufacturing limitations, product heterogeneity, as well as toxicity problems, due to the transfer of a large number of phenotypically diverse T cells. To overcome said limitations, we propose a controlled adoptive cell therapy approach, where T cells are armed with synthetic agonistic receptors (SAR) that are selectively activated by bispecific antibodies (BiAb) targeting SAR and melanoma-associated antigens.

Methods Human as well as murine SAR constructs were generated and transduced into primary T cells. The approach was validated in murine, human and patient-derived cancer models expressing the melanoma-associated target antigens tyrosinase-related protein 1 (TYRP1) and melanoma-associated chondroitin sulfate proteoglycan (MCSP) (CSPG4). SAR T cells were functionally characterized by assessing their specific stimulation and proliferation, as well as their tumor-directed cytotoxicity, in vitro and in vivo.

Results MCSP and TYRP1 expression was conserved in samples of patients with treated as well as untreated melanoma, supporting their use as melanoma-target antigens. The presence of target cells and anti-TYRP1 × anti-SAR or anti-MCSP × anti-SAR BiAb induced conditional antigen-dependent activation, proliferation of SAR T cells and targeted tumor cell lysis in all tested models. In vivo, antitumoral activity and long-term survival was mediated by the co-administration of SAR T cells and BiAb in a syngeneic tumor model and was further validated in several xenograft models, including a patient-derived xenograft model.

Conclusion The SAR T cell-BiAb approach delivers specific and conditional T cell activation as well

WHAT IS ALREADY KNOWN ON THIS TOPIC

⇒ Melanoma has been shown to be sensitive to immunotherapy, though significant subsets of patients do not respond or relapse after initial response.

WHAT THIS STUDY ADDS

⇒ A modular and controllable adoptive T cell therapy approach to the treatment of melanoma.

HOW THIS STUDY MIGHT AFFECT RESEARCH, PRACTICE OR POLICY

⇒ This study puts forward the simultaneous and sequential targeting of melanoma-associated chondroitin sulfate proteoglycan and tyrosinase-related protein 1 as a strategy for the targeted therapy of melanoma.

as targeted tumor cell lysis in melanoma models. Modularity is a key feature for targeting melanoma and is fundamental towards personalized immunotherapies encompassing cancer heterogeneity. Because antigen expression may vary in primary melanoma tissues, we propose that a dual approach targeting two tumor-associated antigens, either simultaneously or sequentially, could avoid issues of antigen heterogeneity and deliver therapeutic benefit to patients.

BACKGROUND

Due to its high tumor mutational burden, likely driven by ultraviolet radiation, melanoma possesses a high number of neoantigens, making it one of the most immunogenic tumor types.^{1 2} Melanoma treatment has been revolutionized by immune check-point blockade (ICB), reactivating T cells or preventing T cell dysfunction.³ Despite these successes, many patients still either do not

respond or relapse after an initial response.⁴ For patients not carrying targetable mutations such as BRAFV600E or having already exhausted targeted treatments, limited options remain, resulting in an urgent need for innovative effective treatments.

While ICB-mediated prevention of T cell dysfunction has entered clinical practice in a wide array of indications beyond melanoma, the direct therapeutic use of T cells in non-hematological cancer entities has been largely ineffective.⁵ Melanoma, however, has been an exception in this regard. Tumor infiltrating lymphocytes (TIL) are a prognostic factor in melanoma and correlate with response to ICB.⁶ In fact, investigation using isolated, non-modified, and ex vivo expanded TIL as a treatment modality for patients with melanoma has already been explored in the pre-ICB era.⁷ There, about 50% of treated patients were sensitive to TIL therapy, a fraction of which exhibiting complete and durable responses.^{8,9} The success of ICB therapy then suspended further development of TIL-based therapies for some time. Recently, clinical studies have explored the potential of TIL therapy after ICB failure in patients with melanoma. Consistent with pre-ICB reports, TIL therapy yielded substantial response rates of up to 32%, indicating that even in such clinically challenging situations, TIL therapy might still be of benefit to patients (NCT00937625, NCT02379195 and NCT02354690).¹⁰ Along these lines, ICB and TIL therapy impressively demonstrate the utility of T cells in melanoma treatment regardless of treatment line. TIL therapy, however, comes with significant challenges which limit its application: (1) requirement for accessible target lesions for resection and TIL selection and expansion, (2) failure to select and expand TIL, (3) heterogeneity of TIL products with often undefined specificities and consequently and (4) heterogeneous response patterns both in extent and in duration.¹¹

T cells can be rendered tumor-specific through genetic engineering of a synthetic receptor, so called chimeric antigen receptor (CAR), that can recognize antigens on the cell surface independent of major histocompatibility complex molecules. Anti-CD19 CAR T cells have entered clinical routine after transformative results in the treatment of hematological malignancies.^{12,13} CD19 as a target antigen allows for targeting of lymphoma and leukemic cells along with healthy B cells. The deleterious effects of depleting the entire B-cell compartment are clinically manageable.¹⁴ In contrast to CD19⁺ hematological malignancies, dispensable lineage-specific tumor-associated antigens are rarely found in solid cancer types.⁵ Additionally, an immunosuppressive milieu and target antigen heterogeneity, among other factors, have resulted in melanoma CAR T cell therapy trials faring poorly thus far.¹⁵ Detailed analysis of TIL therapy failure highlights that loss of dominant antigens under therapeutic pressure happens quite frequently, suggesting that a successful T cell product will need to target more than one antigen.¹⁶ These results support the need for advances in melanoma cell therapy considering such a limitation.

As most of the targetable antigens are not entirely specific to melanoma but shared with other cells as well, we reasoned that any T cell therapeutic strategy would need to be controllable to allow application with a safety net. We have previously described a synthetic agonistic receptor (SAR) platform composed of the extracellular domain of epidermal growth factor receptor variant III (EGFRvIII), fused to intracellular T cell-activating domains (later referred to as E3 construct). The construct can be specifically activated by bispecific antibodies (BiAb) simultaneously targeting the SAR and the tumor antigen. The major advantages of modular adoptive cell therapy (ACT) platforms are the possibility to stop administration of the adaptor molecule in case of undesired therapy-associated toxicities and the ability to target multiple antigens by administering different T cell adaptor molecules.^{17,18} In particular, we previously demonstrated that SAR-transduced T cell activity is conditional to the presence and binding of the BiAb, enabling a tunable activity that is advantageous in case of toxicities.^{19,20} We hypothesized that this SAR platform could serve as a safe and effective way of targeting melanoma-associated antigens for melanoma treatment.²⁰

For the present study, using the CrossMab technology,^{21,22} we developed trivalent BiAb binding melanoma antigen and the E3 SAR. We demonstrate that SAR-transduced T cells were selectively and reversibly activated through the BiAb, solely in the presence of antigen-positive melanoma cells. We showcase substantial activity of the platform in primary melanoma cultures and in several xenograft and syngeneic mouse models, supporting further clinical development.

MATERIAL AND METHODS

Patient and healthy donor material

Frozen, primary and metastatic tumor samples from 13 patients with a histologically confirmed diagnosis of melanoma were used for this study. The samples were cultured in MCDB 153 medium (Merck) complemented with 20% Leibovitz's L-15 medium (Thermo Fisher), 2% fetal calf serum (Gibco), 10 µg/mL human insulin (Merck) and 2 M CaCl₂ solution and expanded until further use. Biological and clinical information were obtained from electronic medical records. Patient characteristics are summarized in online supplemental table 1. Human peripheral blood mononuclear cells (PBMCs) for the generation of human CAR and SAR T cells were isolated from healthy donors by Ficoll density gradient separation.

Mice

Female C57BL/6N and NSG (NOD.Cg-Prkdcscid Il2rgt-m1WjI/SzJ) mice were purchased from Charles River or Janvier Labs. Animals were housed in specific pathogen-free facilities in groups of 2–5 animals per cage. All experimental studies were approved and performed with mice aged 2–4 months and in accordance with guidelines and regulations implemented by the Regierung von

Oberbayern (ROB-55.2–2532.Vet_02-20-208 and ROB-55.2–2532.Vet_02-17-135). In accordance with the animal experiment application, tumor size, behavior, breathing, body weight and posture of mice were monitored three times per week. For survival analyses, the above-described criteria (in particular: curved back, apathy, weight loss >20%, piloerection, pronounced abdominal breathing and cyanosis, spasms, paralysis, tumor size >225 mm² or one of the two measure dimensions >15 mm or open wound in the tumor area) were taken as humane surrogates for survival and recorded in Kaplan-Meier plots.

Animal experiments

MV3, A375 and patient-derived (patient sample 2) xenograft models were established in NSG mice (in total n=96) following the subcutaneous (s.c.) injection of 0.2, 1 or 0.4×10⁶ tumor cells, respectively, in 100 µL phosphate buffered saline (PBS) into the right flank of NSG mice. Syngeneic tumor model was established in C57BL/6 mice (in total n=84) by intravenous injection of YUMM1.1 overexpressing luciferase (and tyrosinase-related protein 1 (TYRP1) where mentioned) (2×10⁶) into the tail vein following a partial lymphodepletion of the B-cell compartment, using 250 µg murine IgG2a anti-CD20 monoclonal antibody (18B12, Roche). Animals were randomized into treatment groups according to tumor burden. Experiments were performed by a scientist blinded to treatment allocation and with adequate controls. No time points or mice were excluded from the experiments presented in the study. For s.c. models, tumor burden was measured three times per week and calculated as mm³ given by volume=(length×width²)/2. Tumor burden of intravenous models were measured using a luciferase-based IVIS Lumina X5 imaging system. For ACT studies, 10⁷ T cells with transduction efficiencies of 50–90% were injected intravenously in 100 µL PBS.

Cell line generation, culture and validation

A375, MV3, PANC-1 and B16 tumor cell lines were purchased from American Type Culture Collection. The ovalbumin overexpressing murine pancreatic cancer cell line Panc02-OVA has been previously described.²⁰ The murine YUMM1.1 cell line was kindly provided by Dr Bosenberg (Yale University, USA). YUMM1.1 tumor cells were stably transduced using retroviral pMP71 vector expressing TYRP1 protein (UNIPROT entry P17643) to generate YUMM1.1 TYRP1 tumor cells. Luciferase-eGFP (LUC-GFP) overexpressing cell line YUMM1.1 TYRP1-LUC-GFP and YUMM1.1 LUC-GFP were generated according to a previously described protocol.²⁰ All tumor lines were grown as previously described,²⁰ and used for experiments when in the exponential growth phase.

Virus production

293Vec-Galv, 293Vec-Eco and 293Vec-RD114 were a kind gift of Manuel Caruso, Québec, Canada, and have been previously described.²³ For virus production, retroviral pMP71 (kindly provided by C. Baum, Hannover) vectors

carrying the sequence of the relevant receptor were stably introduced in packaging cell lines. Single cell clones were generated and indirectly screened for virus production by determining transduction efficiency of primary T cells. This method was used to generate the producer cell lines 293Vec-RD114 for EGFRvIII-CD28-CD3ζ (E3), EGFRvIII with CD28 transmembrane domain lacking intracellular signaling domains (E3del) and anti-HER2-CD28-CD3ζ (HER2 CAR). 293Vec-Galv, 293Vec-Eco and 293Vec-RD114 were grown as previously described.²⁴ All cell lines used in experiments were regularly checked for mycoplasma species with the commercial testing kit MycoAlert (Lonza). Authentication of human cell lines by STR DNA profiling analysis was conducted in house.

T cell generation, retroviral transduction and culture

Human and murine SAR construct generation was previously described.²⁰ SAR-transduced T cells will be referred to as SAR T cells. The HER2 CAR was generated with a humanized single-chain variable fragment against HER2 (4D5).²⁵ Murine T cells were differentiated from splenocytes from donor mice. T cell isolation and transduction protocols have been previously described.²⁶ T cells were expanded or directly expanded with T cell medium supplemented with human interleukin (IL)-15 (PeproTech) every second day. Human T cells have been differentiated and transduced using previously described protocols²⁷ or directly taken into culture with human T cell medium in concentrations of 10⁶ T cells per mL medium.

Cytotoxicity assays

For impedance-based real-time killing assays using a xCELLigence system (ACEA Bioscience), previously described,²⁰ 10⁴ tumor cells were seeded per well in a 96-well plate. Cell number was monitored over the time frame of 10 hours for every 20 min. 10⁵ T cells transduced with the indicated receptors were added to the tumor cells. For lactate dehydrogenase (LDH)-based killing assays, T cells were incubated with tumor cells and BiAb at indicated effector to target ratios and concentrations. Transduced T cells were added to the adherent tumor cells and co-cultured as indicated. LDH levels were measured according to the manufacturer's protocol (Promega). Additionally, the killing of melanoma patient samples was assessed using a flow cytometry-based readout after 48 hours of co-culture with human SAR T cells in the presence of either the anti-TYRP1/anti-EGFRvIII (αTYRP1/αE3) which is cross-reactive to human and murine TYRP1 or the anti-human melanoma-associated chondroitin sulfate proteoglycan (MCSP, also known as CSPG4)/anti-EGFRvIII BiAb (αMCSP/αE3). Tumor cells were stained with the cell proliferation dye eFluor 450 according to the manufacturer's protocol (eBioscience). Depending on the tumor cell size 2–4×10⁴ cells per well were co-cultured with SAR T cells in an effector to target cell ratio of 2:1 in a 96-well plate. Tumor cells were detached using trypsin. Dead cells were stained using the violet fixable

viability dye (BioLegend) for 15 min at room temperature. Following this, cell surface proteins were stained for 20 min at 4°C. For the characterization and quantification of the SAR T cells antibodies against CD3 (OKT3), CD4 (OKT4), CD8a (RPA-T8), PD-1 (EH12.2H7), 4-1BB (4B4-1), CD69 (FN50) and EGFR (A-13) (all from BioLegend) were used. Tumor and T cell counts were normalized to counting beads (Invitrogen).

Proliferation assays

SAR T cell proliferation was measured using a flow cytometry-based assay that compared fold proliferation of CD3⁺ (17A2, BioLegend) T cells over a period of 48 hours normalized to the number of T cells per bead at indicated concentrations and effector to target ratio.

Biodistribution study

For the biodistribution study of the anti-TYRP1/anti-E3 BiAb (α TYRP1/ α E3 BiAb), 2×10^6 YUMM1.1 TYRP1-LUC-GFP tumor cells were intravenously injected into C57Bl/6 mice. IVIS imaging was used to verify tumor engraftment and distribution after 13 and 20 days. α TYRP1/ α E3 or α Mesothelin/ α E3 control BiAb (5 μ g/mouse or 10 mg/kg) were injected intraperitoneally (i.p.) into tumor-bearing (for each antibody $n=3$) and non-tumor-bearing mice (for each antibody $n=2$) on day 20. Experimental readout was taken 48 hours later. In addition to the metastasis in the lung, organs with the highest TYRP1 expression relative to baseline (skin and heart) were also harvested. Organ tissue was embedded and frozen in optimal cutting temperature compound before preparation for immunofluorescence staining and imaging.

Immunofluorescence

The 5 μ m tissue cryosections were stained on chip cytometry slides (Zellkraftwerk) with an antibody (polyclonal, AF555, Thermo Fisher Scientific) against the human IgG1-based α TYRP1/ α E3 BiAb, a rabbit anti-GFP antibody (polyclonal, Novus Biologicals), a secondary antibody against rabbit IgG (polyclonal, PerCP, Jackson ImmunoResearch) and Hoechst 33342 (Thermo Fisher Scientific). The fluorescence was measured using the ZellScannerONE (Zellkraftwerk).

PCR and quantitative real-time PCR

All DNA constructs were generated by overlap extension PCR²⁴ and recombinant expression cloning into the retroviral pMP71 vector²⁰ using standard molecular cloning protocols.²⁶ RNA was extracted from cells using the InviTrap Spin Universal RNA extraction Kit (Stratag). Complementary DNA was synthesized using the SuperScript II kit (Life Technologies). Real-time PCR reactions were performed using SYBR Green PCR Master Mix (Applied Biosystems) and sequence specific primers for human MCSP, human and murine TYRP1.^{28–30} The amplification was performed with CFX Connect Real-Time PCR Detection System (Bio-Rad Laboratories) running up to 50 cycles of 5 s at 95°C followed by 30 s at 60°C after

an initial step of 95°C for 2 min. Melting curves from 65°C to 95°C were performed to evaluate the specificity of the PCR. The messenger RNA (mRNA) expression levels of human TYRP1 and MCSP were normalized to the expression of phosphoglycerate kinase. The mRNA expression levels of murine TYRP1 were normalized to the expression of β -actin.

Cytokine release assays

Murine and human SAR T cell stimulation assays were set-up at indicated concentrations and effector to target ratios. Murine SAR T cells were co-cultured with B16, YUMM1.1 TYRP1 and Panc02-OVA cell lines. Human SAR T cells were co-cultured with MV3, A375 cell lines and human melanoma samples. Cytokine quantification was measured by ELISA for the following: interferon (IFN)- γ (BD), IL-2 (BD), tumor necrosis factor (TNF)- α (R&D Systems) and granzyme B (R&D Systems).

Statistical analysis

Two-tailed student's t-test was used for comparisons between two groups, while two-way analysis of variance with Bonferroni post-test (multiple time points) was used for comparisons across multiple groups. A log-rank (Mantel-Cox) test was used to compare survival curves. All statistical tests were performed with GraphPad Prism V.8 software, and $p < 0.05$ was considered statistically significant and represented as * $p < 0.05$, ** $p < 0.01$ and *** $p < 0.001$. No statistical methods were used to predetermine sample size. Investigators were blinded to treatment allocation during experiments and outcome assessment.

RESULTS

MCSP and TYRP1 are differentially expressed in melanoma

To identify suitable target structures, we assessed the expression of TYRP1 and MCSP in human melanoma cell lines as well as melanoma samples from treated and untreated patients. Both genes were shown to be highly expressed in melanoma relative to PBMC and human pancreatic cancer cell line PANC-1 control samples both at RNA and protein level (figure 1A–C, online supplemental figure 1A, online supplemental table 1). Analysis of The Cancer Genome Atlas RNA sequencing (RNA-seq) expression data also revealed MCSP to be differentially regulated in cutaneous melanoma tissue relative to skin tissue from healthy donors (figure 1D). Although the median expression of TYRP1 in cutaneous melanoma tissue was similar to the expression in skin from healthy donors, there was a far greater variability in its expression in patients with melanoma with a clear differential expression in a subset of patients (figure 1D). The expression of the targets was also analyzed across different cell types within the same patient (figure 1E), taking advantage of a single cell RNA-seq data set—GSE72056 of 3993 cells from 19 patients,³¹ which revealed a distinct, only partially overlapping pattern of expression for each antigen in tumor tissue (figure 1F and G). Furthermore,

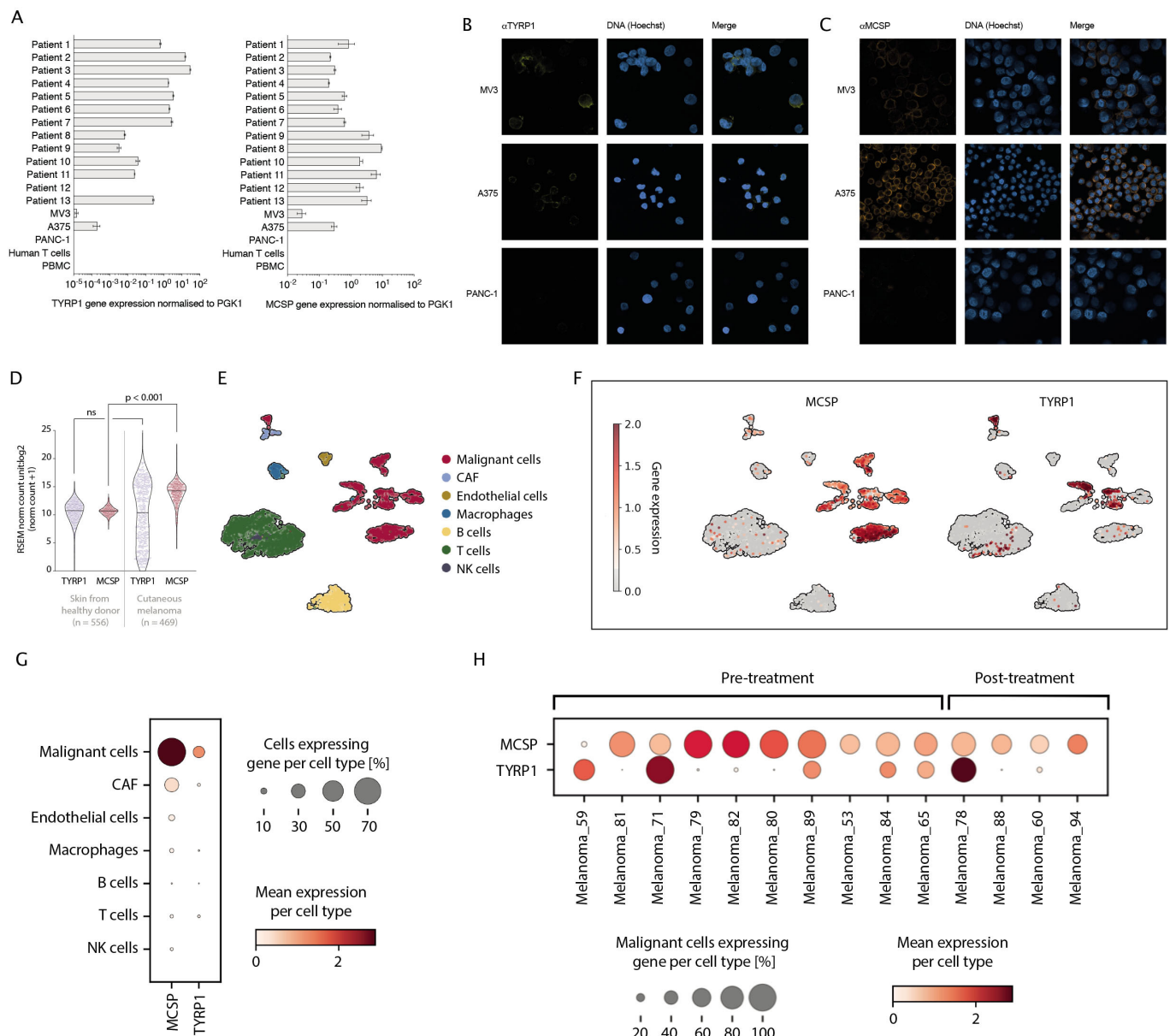


Figure 1 MCSP and TYRP1 are differentially expressed on melanomas. (A) RT-PCR MCSP and TYRP1 gene analysis of human melanoma cell lines, patient-derived melanomas and controls. (B) Microscopic analysis of TYRP1 expression on permeabilized MV3, A375 and PANC-1 cells using αTYRP1/αE3 BiAb (αTYRP1) and anti-human IgG secondary antibody. (C) Microscopic analysis of MCSP expression on MV3, A375 and PANC-1 cells using αMCSP/αE3 BiAb (αMCSP) and anti-human IgG secondary antibody. (D) TCGA analysis of RNA-seq expression of TYRP1 and MCSP in skin from healthy donors and cutaneous melanoma (cutaneous melanoma: n=469; skin from healthy donor: n=556). Scales are depicted in a log2 scale and messenger RNA normalization was estimated by the TCGA using the RSEM (RNA-seq by expectation maximization) method. (E) UMAP showing 3993 (following quality control) healthy and malignant cells from 19 previously published patients (GSE72056). Normalized gene expression values were logarithmized. Colors highlight the different cell types. Annotations of cells were provided by the authors of the respective study. (F) Expression of MCSP and TYRP1 in different cell types. Normalized gene expression values were log-transformed and visualized in a UMAP embedding. (G) Expression of MCSP and TYRP1 per cell type. Color intensity indicates mean gene expression per cell type, dot size indicates the proportion of cells expressing the respective gene per cell type. Normalized expression values were log-transformed. (H) Expression of MCSP and TYRP1 across 14 samples from melanoma patients pre-treatment or post-treatment. Color intensity indicates mean gene expression per patient, dot size indicates the proportion of malignant cells expressing the respective gene per patient. Normalized expression values were log-transformed. Statistical analysis in (D) was performed with the unpaired two-tailed Student's t-test. Experiments in subfigure (A) show mean values±SD calculated from three replicates, violin plots and the median values in (D) calculated from n independent biological replicates. Experiments in subfigures (B) and (C) show one representative of two independent experiments. CAF, cancer-associated fibroblast; MCSP, melanoma-associated chondroitin sulfate proteoglycan; NK, natural killer; PBMC, peripheral blood mononuclear cell; PGK1, phosphoglycerate kinase 1; RNA-seq, RNA sequencing; TCGA, The Cancer Genome Atlas; TYRP1, tyrosinase-related protein 1; RSEM, RNA-seq by expectation maximization.

MCSP expression on malignant cells was well-maintained in patients that received treatment (figure 1H). TYRP1 expression pattern was similar in pre-treatment and post-treatment samples but characterized by a high spread (figure 1H).

α MCSP/ α E3 and α TYRP1/ α E3 BiAb bind MCSP⁺ and TYRP⁺ melanoma cells

BiAb-mediated T cell activation is dependent on antibody aggregation on the target cell before their presentation to T cells in a polyvalent form. Our previous work on the SAR platform could show that BiAb must have a single specificity for E3 to ensure conditional SAR T cell activation in the presence of the target antigen.²⁰ This informed the BiAb design used in this study, with a trivalent and bispecific format with two specificities for the tumor antigen (TYRP1 or MCSP) and a single specificity for E3 (online supplemental figure 1B,C). The binding properties and apparent dissociation constant (K_D) of BiAb (anti-MCSP/anti-E3 BiAb (α MCSP/ α E3) and anti-TYRP1/anti-E3 BiAb (α TYRP1/ α E3)) to both their targets (online supplemental figure 1D,E) and EGFRvIII (online supplemental figure 1F) were analyzed by flow cytometry. The previously characterized α Mesothelin/ α E3 BiAb binding the SAR and mesothelin was used as a non-melanoma targeting control construct in subsequent experiments.²⁰

α MCSP/ α E3 and α TYRP1/ α E3 BiAb can mediate SAR T cell activation, proliferation and differentiation

SAR constructs could be retrovirally transduced into primary murine and human T cells with high efficiencies (figure 2A). Following transduction and expansion protocols, CD4⁺ and CD8⁺ human SAR T cells were shown to be of similar frequencies and to predominantly have an effector memory phenotype (figure 2B,C). We assessed SAR T cell activation and cytokine release in both murine and human T cells. For murine T cells, we incubated SAR T cells with two TYRP1-expressing cell lines, B16 and YUMM1.1 TYRP1 and with the antigen-negative, pancreatic cancer cell line Panc02-OVA (online supplemental figure 1G–I) in the presence of α TYRP1/ α E3 BiAb. Murine SAR T cells specifically released IFN- γ , IL-2, TNF- α and granzyme B and expressed the activation markers programmed cell death protein 1 (PD-1) and CD69 on co-culture with TYRP1⁺ melanoma cell lines, unlike in co-culture with antigen-negative Panc02-OVA tumor cells (online supplemental figure 2A,B). SAR T cells only proliferated in the presence of TYRP1-expressing tumor cells and BiAb (online supplemental figure 2C). Human SAR T cells were incubated with the MCSP⁺ and TYRP1⁺ cell lines, A375 and MV3, respectively. Only in the presence of the MCSP-targeting BiAb molecule and the target antigen, human SAR T cells released IFN- γ , IL-2, TNF- α and granzyme B. In contrast, untransduced T cells (Unt) and control-E3del-transduced T cells remained inactive and did not produce cytokines or cytotoxic granules regardless of the presence of the BiAb and target

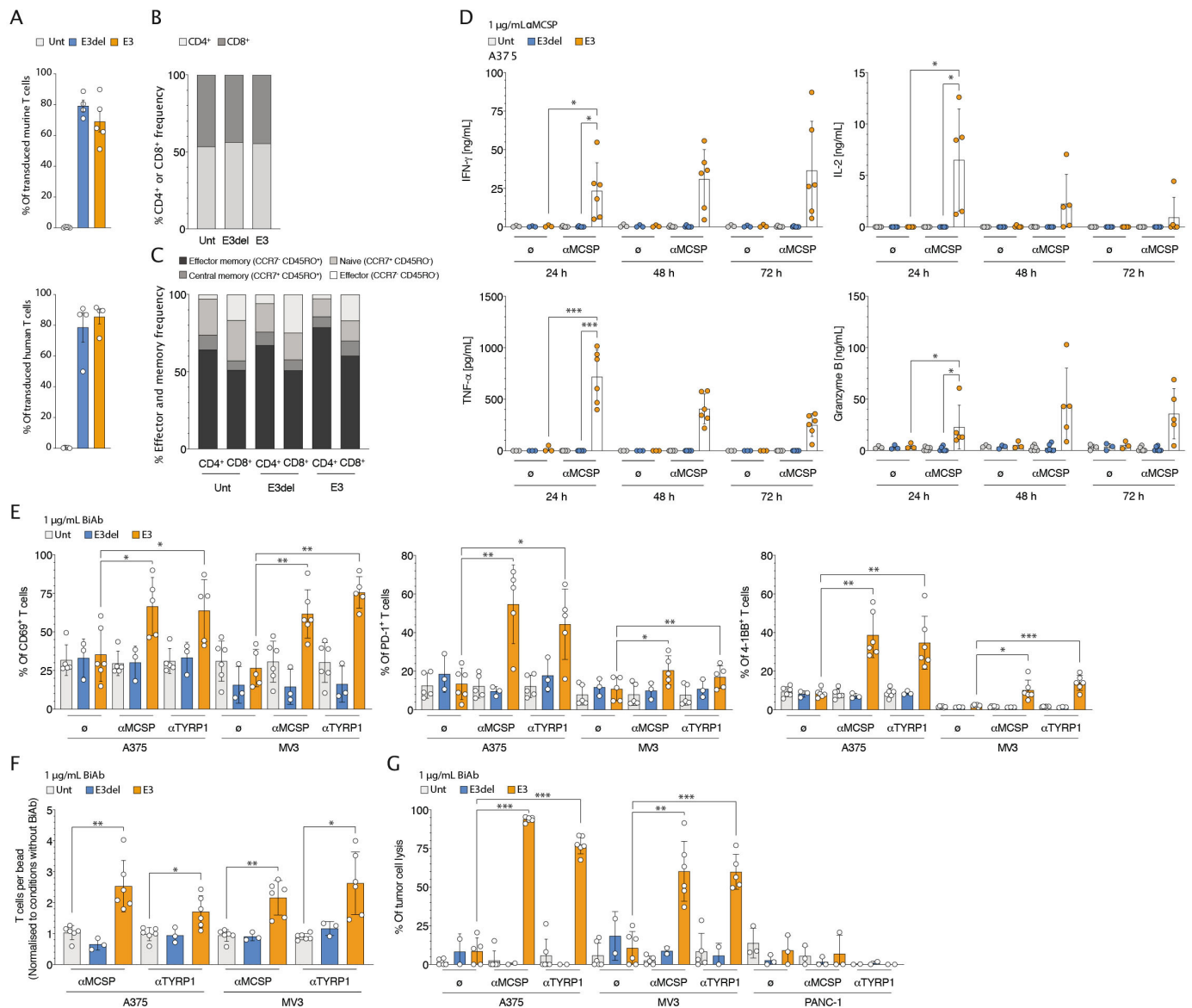
antigen (figure 2D). The frequency of CD69, PD-1 and 4-1BB-expressing SAR T cells was increased in the presence of either one of the two BiAb molecules and antigen-expressing target cells (figure 2E). CD4⁺ and CD8⁺ T cell proliferation was congruent with the activation observed, as stimulated SAR T cells proliferated more than control T cells or SAR T cells in the absence of BiAb (figure 2F).

SAR T cells can target and lyse MCSP-expressing and TYRP1-expressing melanomas

Using flow cytometry-based and impedance-based assays, we evaluated whether SAR T cells could selectively lyse MCSP-expressing and TYRP1-expressing melanoma cells in the presence of a bridging BiAb. Human SAR T cells specifically eliminated antigen-positive A375 and MV3 melanoma cells when co-cultured together with either an α MCSP/ α E3 or α TYRP1/ α E3 BiAb whereas no lysis was detected with the antigen-negative pancreatic cancer cell line PANC-1 (figure 2G). Similarly, murine SAR T cells only lysed TYRP1⁺ B16 and YUMM1.1 TYRP1 melanoma cells in the presence of an α TYRP1/ α E3 BiAb (online supplemental figure 2D,E). TYRP1-specific and MCSP-specific BiAb conditionally activated human SAR T cells in co-culture with patient-derived melanoma samples. SAR T cells showed increased expression of the activation markers CD69, PD-1 and 4-1BB, secretion of IFN- γ and proliferation, relative to E3 only or Unt T cell in presence of either of the BiAb (figure 3A–C). Also, TYRP1-specific and MCSP-specific BiAb redirected SAR T cells to target and lyse all patient-derived melanoma samples tested, whereas Unt and BiAb controls had no effect on tumor cell lysis (figure 3D).

Cleavable proteins do not impact SAR-BiAb platform efficacy and safety

With elevated levels of MCSP having been reported in the sera of patients with melanoma,³² we sought to better understand the potential impact of soluble MCSP or TYRP1 on the SAR T cell-BiAb approach. Therefore, soluble recombinant MCSP and TYRP1 proteins were used. Proteins were added in ascending concentrations to a T cell-tumor cell co-culture to study T cell killing efficiency and kinetics. Ascending concentrations of MCSP and TYRP1, including concentrations at a physiological level, did not impair SAR T cell killing (figure 4A and online supplemental figure 3A). We also sought to test whether free soluble protein targets would induce unwanted off-tumor SAR T cell activation. We found that soluble MCSP and TYRP1 did not induce SAR T cell activation in the presence of either relevant BiAb, both at physiological and supraphysiological concentrations that were tested. There, no significant changes in IFN- γ levels were observed when comparing E3 and BiAb conditions to controls containing soluble recombinant MCSP or TYRP1 (figure 4B and online supplemental figure 3B). It should be noted that in this setting a higher basal SAR T cell activation was



observed with the α TYRP1/ α E3 compared with the α MCSP/ α E3 BiAb. It appears that the SAR T cell-BiAb platform is not easily impacted by alternative soluble sources of targeted proteins and requires

immobilization of these on the tumor cell surface, as previously described for other targets in one of our previous studies.²⁰ These findings align with the fact that the BiAb was designed only to bind a

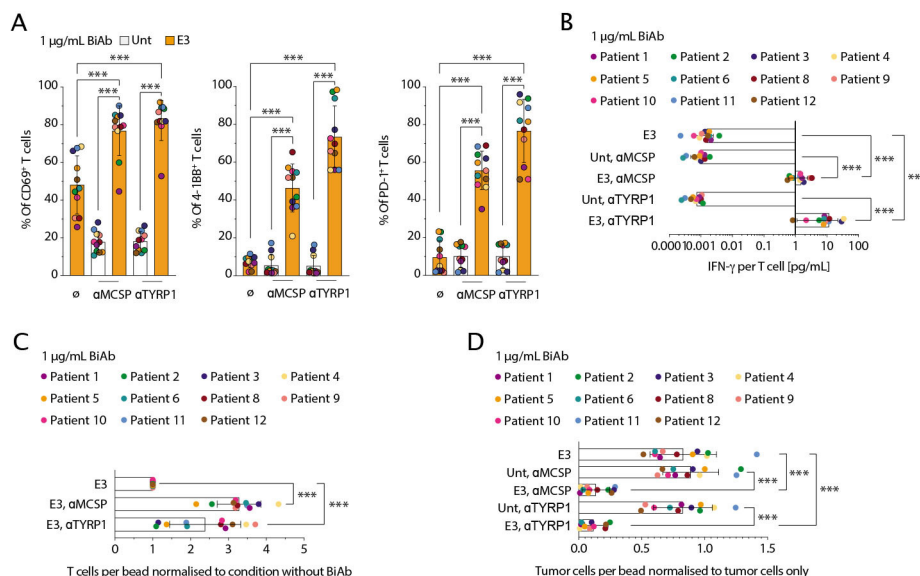


Figure 3 αMCSP/αE3 and αTYRP1/αE3 BiAb activate SAR T cells to mediate specific cytotoxicity against patient-derived melanoma samples. (A) Human T cells were co-cultured with patient-derived melanoma samples (effector to target ratio 2:1) and either αMCSP/αE3 or αTYRP1/αE3 BiAb (αMCSP or αTYRP1, 1 μg/mL) for 48 hours. The frequency of CD69, PD-1 and 4-1BB on T cells was assessed using flow cytometry. (B) Supernatant was taken and analyzed with ELISA for IFN-γ. The values were normalized to the numbers of plated T cells. (C) The CD3⁺ T cell count per bead was measured and normalized to conditions without BiAb. (D) The percentage lysis of the patient-derived melanoma samples by SAR T cells and either of the two BiAb was calculated based on flow cytometric readout after 48 hours of co-culture. The values shown were normalized to the tumor cells only control conditions. Statistical analysis was performed using the paired two-tailed Student's t-test. Experiments show mean values ± SD. Each data point represents the mean of 2–3 biological replicates. BiAb, bispecific antibodies; IFN, interferon; MCSP, melanoma-associated chondroitin sulfate proteoglycan; PD-1, programmed cell death protein 1; SAR, synthetic agonistic receptor; TYRP1, tyrosinase-related protein 1; Unt, untransduced T cells.

membrane-proximal epitope that remains on the cell surface following cleavage.

Modular, selective and reversible activation of SAR T cells against melanoma

Melanomas are heterogeneous and stand to benefit from a modular and controllable therapeutic approach. Use of the melanoma differentiation antigens shared with other cells calls for control over these effects to antagonize potential unwanted excessive toxicities. While classic CAR T cell activity is maintained in the presence of a target antigen, SAR T cell activation is modular and controllable (figure 4C).¹⁹ To demonstrate this in the melanoma setting, we used an in vitro stimulation assay to show how BiAb-dependent SAR activation enables greater control over T cell function (online supplemental figure 3C). As expected, following a 24-hour co-culture with MCSP⁺ TYRP1⁺ A375 tumor cells, SAR T cells could be activated in the presence of either of the two BiAb molecules (figure 4D). The same SAR T cells were then transferred to a new plate containing freshly plated A375 cells where they were co-cultured for a further 24 hours under different stimulation conditions. We found IFN-γ expression was maintained when SAR T cells were redosed with either one of the two BiAb molecules (figure 4E). However, the concentration of IFN-γ decreased in the absence of BiAb redosing, indicating the reversibility of SAR T cell activation. This was distinct from the lack of controllability seen with human anti-HER2 CAR T cells

when targeting HER2⁺ A375 tumor cells, which continued to sense HER2⁺ tumor cells³³ (figure 4E).

At the same time, sequential targeting of multiple antigen types would allow for more refined patient-specific tailoring of treatment and prevention of antigen-negative relapse. Through redosing with αMCSP/αE3 BiAb (first dosing with αTYRP1/αE3), the transferred SAR T cells remained activated, as shown by an elevated IFN-γ concentration after 48 hours of co-culture (figure 4E).

By sequentially redirecting SAR T cells towards different melanoma targets with high efficiency, the modularity of the platform was demonstrated (figure 4D, E). Overall, this approach has the potential to target a variety of melanoma-associated antigens with a level of flexibility and controllability that is superior to that of CAR T cells.

SAR T cell-BiAb combination mediates effective tumor control in vivo

To probe the in vivo function of the SAR T cell-BiAb combination, we established and used both syngeneic and xenograft melanoma models. We engrafted the YUMM1.1 TYRP1-LUC-GFP murine melanoma cell line into C57BL/6 mice. The MV3 and A375 human melanoma cell lines and a sample from a patient with primary melanoma (sample 2) were implanted into NSG mice. In the syngeneic model, following adoptive transfer, SAR T cells were shown to persist well, where SAR⁺ T cells could be tracked in the peripheral blood of mice at 7, 14 and 19 days post transfer (online supplemental figure 4A).

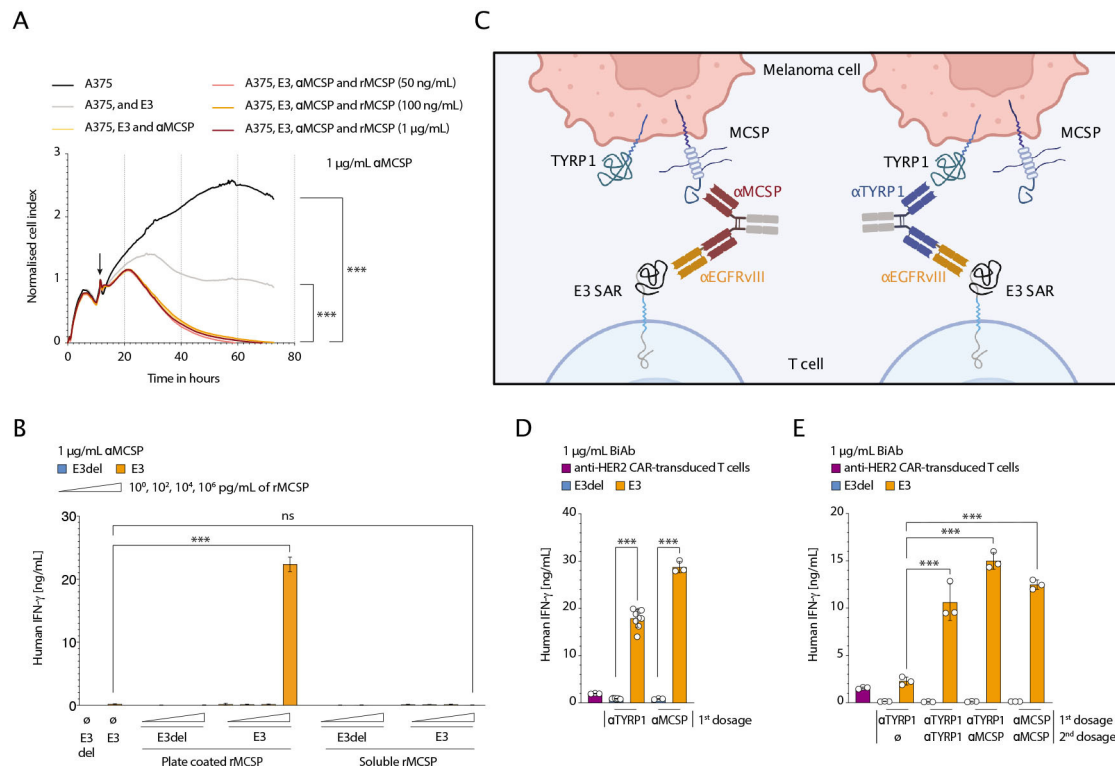


Figure 4 Modular, selective and reversible activation of SAR T cells, irrespective of soluble forms of MCSP tumor antigen. (A) A375 melanoma cells were plated and co-cultured with human SAR T cells (E:T 2:1) and αMCSP/αE3 BiAb (αMCSP, 1 μg/mL). Different concentrations of soluble, recombinant MCSP (rMCSP) were added. The tumor cell lysis over time was assessed using xCELLigence (n=3). The cell index was normalized to the respective time point of T cell addition as indicated by an arrow. (B) Human SAR or E3del control T cells and αMCSP/αE3 BiAb (1 μg/mL) were plated in wells either coated with different concentrations of rMCSP or where different concentrations of soluble rMCSP were added to the medium. After 48 hours the supernatant was taken and analyzed for IFN-γ using ELISA (n=3). (C) Schematic overview of SAR-transduced T cells targeting TYRP1⁺ MCSP⁺ melanoma cells via an αTYRP1/αE3 or αMCSP/αE3 BiAb. (D and E) A modularity stress test was carried out using αMCSP/αE3 or αTYRP1/αE3 BiAb (αMCSP or αTYRP1, 1 μg/mL). SAR or E3del control T cells were co-cultured with A375 tumor cells (E:T 2:1). HER2 CAR T cells were used as a control and co-cultured with HER2⁺ A375 tumor cells (no BiAb was added). At assay start, co-cultures received either αMCSP/αE3 or αTYRP1/αE3 BiAb (first dosage). At 24 hours, the T cells were washed to remove residual BiAb and transferred to freshly plated A375 tumor cells. Co-cultures were then either redosed with the same BiAb, redosed with the BiAb against the other target, or not redosed after initial dosing (second dosage) and incubated for another 24 hours. At 24 (D) or 48 hours (E), supernatants were taken and ELISA for human IFN-γ were performed (n=3). Analyses of differences between groups for (A) were performed using two-way analysis of variance with correction for multiple testing by the Bonferroni method. For statistical analysis of (B), (D) and (E), the unpaired two-tailed Student's t-test was used. Experiments show mean values±SD calculated from at least three biological replicates and are representative of three independent experiments. BiAb, bispecific antibodies; E:T, effector to target ratio; IFN, interferon; EGFRvIII, epidermal growth factor receptor variant III; MCSP, melanoma-associated chondroitin sulfate proteoglycan; SAR, synthetic agonistic receptor; TYRP1, tyrosinase-related protein 1; HER2, human epidermal growth factor receptor.

Mice that were treated with SAR T cells and repeated αTYRP1/αE3 BiAb dosing were able to clear the disease and achieved long-term survival (4 out of 10 mice with a complete response) (figure 5A,B, online supplemental figure 4B). In an endpoint experiment (19 days after T cell transfer) the lungs were harvested and analyzed using flow cytometry. SAR T cell and repeated αTYRP1/αE3 BiAb combination treatment led to a complete tumor clearance in four out of five mice based on a flow cytometry and IVIS readout (figure 5C and online supplemental figure 4C). In contrast, a single dose of the αTYRP1/αE3 BiAb in combination with SAR T cells only showed transient tumor control and did not lead to tumor clearance nor prolonged survival of the treated mice (online

supplemental figure 4D,E), indicating the necessity for redosing for maintained SAR activity in vivo. This necessity for redosing demonstrates a reversibility in SAR T cell activity on dosing cessation.

In order to analyze the antigen-specificity of the approach in vivo, mice bearing antigen-negative YUMM1.1 LUC-GFP tumors were treated with SAR T cell-BiAb combination. Treatment of antigen-negative tumors did not impact tumor growth and survival compared with control mice treated with SAR T cells or the vehicle solution (online supplemental figure 4F,G) underpinning the necessity of target antigen expression for the functionality of the approach. To further analyze the specificity of the αTYRP1/αE3 BiAb, TYRP1-expressing organs

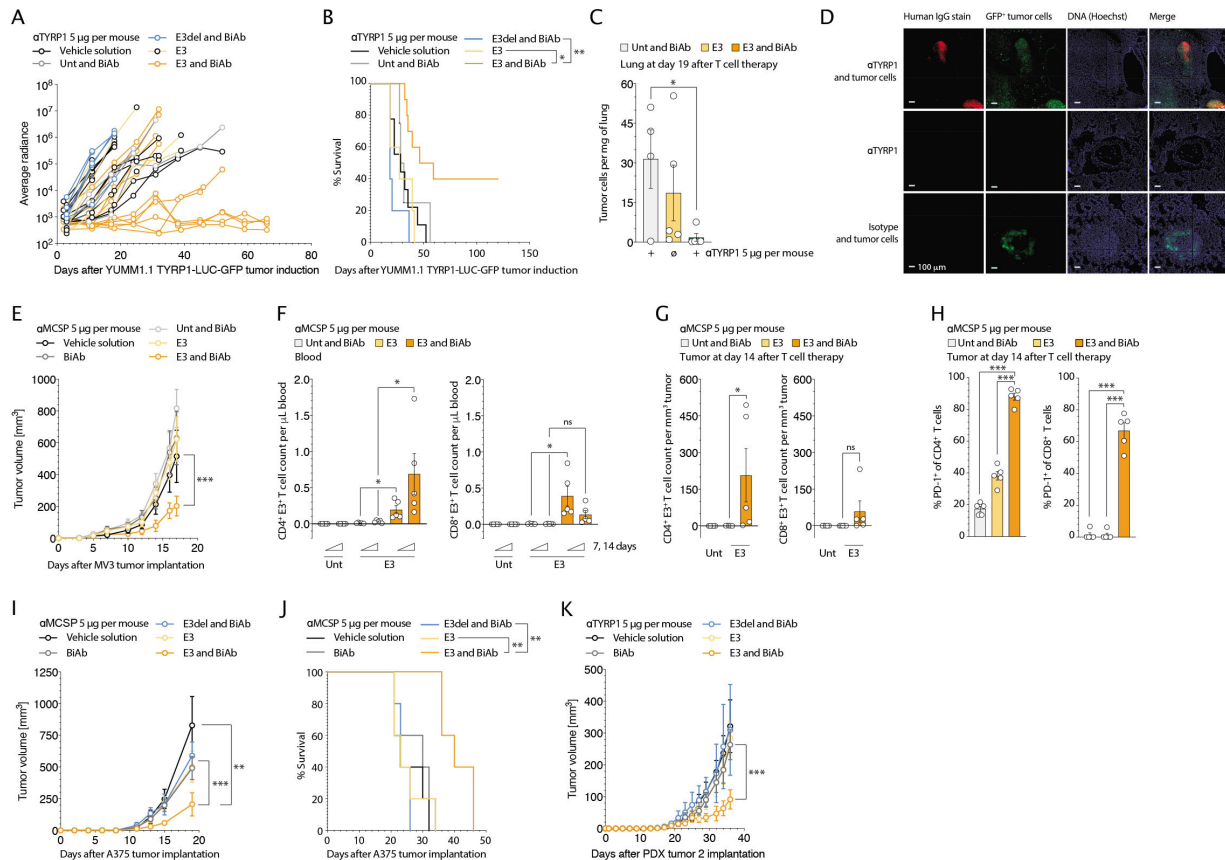


Figure 5 Treatment with the SAR T cell-BiAb combination is effective in syngeneic and xenograft melanoma models and enhances survival in vivo. (A) C57BL/6 mice were injected i.p. weekly with an anti-CD20 depleting antibody (250 µg/injection) starting 7 days before tumor cell injection. Mice were inoculated intravenously with 2×10^6 YUMM1.1 TYRP1-LUC-GFP tumor cells. Mice were treated with a single intravenous injection of T cells 4 days after tumor cell injection. Simultaneously, antibody treatment was given by i.p. injections of the α TYRP1/ α E3 BiAb (α TYRP1, 5 µg/injection) which was redosed two times per week. In vivo luminescent signal imaging was performed one time per week using IVIS. Treatment groups were as follows: SAR T cells and α TYRP1/ α E3 BiAb (n=10), E3del T cells and α TYRP1/ α E3 BiAb (n=5), SAR T cells (n=5), Unt T cells and α TYRP1/ α E3 BiAb (n=4), and the vehicle solution (n=9). (B) Percentage survival readout. (C) Tumor burden per mg of lung tissue 19 days after T cell therapy using a flow cytometry-based readout. Mice were treated with either SAR T cells and α TYRP1/ α E3 BiAb (n=5), Unt T cells and α TYRP1/ α E3 BiAb (n=4) or SAR T cells only (n=5) 4 days after tumor induction. (D) Immunofluorescence imaging of the α TYRP1/ α E3 BiAb and tumor cell-derived GFP in lung tissue was carried out with anti-human IgG and anti-GFP stainings. Mice were injected intravenous either with 2×10^6 YUMM1.1 TYRP1-LUC-GFP cells or with vehicle solution. After 20 days the mice were injected either with 5 µg α TYRP1/ α E3 BiAb, an isotype BiAb or with the vehicle solution. Following 48 hours of incubation, the lung, heart and skin were harvested, stained and imaged using ZellScannerONE. The groups were as follows: Tumor and α TYRP1/ α E3 BiAb (n=3), α TYRP1/ α E3 BiAb only (n=2), tumor and isotype BiAb (n=3). (E) NSG mice were inoculated s.c. with 1×10^6 MV3 tumor cells. Mice were treated with a single intravenous injection of T cells 5 days after tumor cell injection. Simultaneously, antibody treatment was given by i.p. injections of the α MCSP/ α E3 BiAb (α MCSP, 5 µg/injection) which was redosed two times per week. Treatment groups were as follows: SAR T cells and the α MCSP/ α E3 BiAb (n=5), Unt T cells and α MCSP/ α E3 BiAb (n=4), SAR T cells only (n=5), BiAb only (n=5), and the vehicle solution (n=5). (F) In an endpoint experiment, SAR T cell persistence in the blood and in the tumor was analyzed using a flow cytometry-based readout 14 days after T cell transfer. The mice were treated with either SAR T cells and α MCSP/ α E3 BiAb, Unt T cells and α MCSP/ α E3 BiAb or SAR T cells only (for each group n=5). (G) SAR T cell infiltration per mm³ tumor. (H) Frequency of PD-1 expression on human CD4⁺ and CD8⁺ T cells in the tumor. (I) NSG mice were injected s.c. with 0.2×10^6 A375 tumor cells. The mice were treated according to the experiment in (E) 11 days after tumor induction (for E3del and α MCSP/ α E3 BiAb: n=4, for other groups: n=5). (J) Percentage survival readout. (K) NSG mice were injected s.c. with 0.4×10^6 patient-derived melanoma cells (patient sample 2). The mice were treated according to the experiment in (E) 12 days after tumor induction with α TYRP1/ α E3 BiAb (for E3del and α TYRP1/ α E3 BiAb, and vehicle solution: n=4, for other groups: n=5). For statistical analysis of survival data, the log-rank test was applied. Analyses of differences between groups for (E), (I) and (K) were performed using two-way analysis of variance with correction for multiple testing by the Bonferroni method. For statistical analysis of (C), (F), (G) and (H) the unpaired two-tailed Student's t-test was used. Experiments show mean values \pm SEM calculated from n biological replicates, one experiment for (B), (C), (F), (G), (H) and (K), and one representative of two independent experiments in (A), (E), (I) and (J). BiAb, bispecific antibodies; i.p., intraperitoneally; MCSP, melanoma-associated chondroitin sulfate proteoglycan; PD-1, programmed cell death protein 1; PDX, patient-derived xenograft; SAR, synthetic agonistic receptor; s.c., subcutaneously; TYRP1, tyrosinase-related protein 1; Unt, untransduced T cells.

(heart and skin) and tumor-bearing lungs were harvested 48 hours after BiAb injection and the BiAb was stained using immunofluorescence. α TYRP1/ α E3 BiAb specifically bound to YUMM1.1 TYRP1-LUC-GFP tumor cells in the lung, while no comparable binding of the BiAb could be detected in other TYRP1-expressing tissues, indicative of its selectivity for melanoma cells (figure 5D and online supplemental figure 4H).

In the human MV3 xenograft model, a strong antitumoral response was again observed in the group treated with SAR T cells and α MCSP/ α E3 BiAb compared with all controls (figure 5E). In this group, durable persistence of SAR-transduced T cells was seen by flow cytometry at 7 and 14 days post transfer (figure 5F). At the experimental endpoint, tumors were harvested and analyzed by flow cytometry. Higher numbers of tumor infiltrating SAR T cells were found in mice that received the SAR T cell-BiAb treatment combination (figure 5G), with CD4⁺ T cells persisting better than CD8⁺ T cells in contrast to any of the controls. Phenotyping of transferred T cells at the experimental endpoint revealed maintenance of the effector memory phenotype they had prior to adoptive transfer (as determined by CD45RO and CCR7 expression) (online supplemental figure 4I). Furthermore, PD-1 expression was increased in SAR T cell-BiAb treated mice compared with SAR T cell only or Unt T cells and BiAb control conditions (figure 5H). Similar to the MV3 model, the A375 xenograft model, demonstrated comparable sensitivity to SAR T cells and BiAb resulting in improved tumor control and prolonged survival (figure 5I and J). Additionally, in a patient-derived xenograft model, treatment with the α TYRP1/ α E3 BiAb and SAR T cells resulted in reduced tumor growth in mice receiving SAR T cell and BiAb combination (figure 5K).

DISCUSSION

We could demonstrate that MCSP and TYRP1 expression remains differentially expressed on primary melanoma samples of patients pre-treatment or post-treatment. We reasoned that their targeting using a modular and controllable T cell therapy platform, in the form of the SAR T cell-BiAb approach, could be an effective strategy and probed this hypothesis in vitro and in vivo. In order to demonstrate the translational relevance of the approach, we selected a series of relevant in vitro and in vivo models. We used immunocompetent syngeneic mouse models to better control for the immune system's impact on the treatment approach and primary human melanoma models and cell lines to test the efficacy of the approach in treated as well as untreated melanoma models.

Our results demonstrate the efficacy of the approach in several in vitro and in vivo models. SAR-engineered T cells could be redirected towards MCSP-expressing and TYRP1-expressing melanoma cells in the presence of the α MCSP/ α E3 or α TYRP1/ α E3 BiAb. SAR T cells efficiently targeted and lysed MCSP-expressing and TYRP1-expressing melanoma cell lines. Targeted specificity and

killing capacity were retained when targeting patient-derived melanomas, using in vitro co-cultures, as well as several syngeneic and xenograft in vivo mouse models.

The potent cytolytic effects of the platform in the syngeneic model resulted in 4 out of 10 mice completely curing the tumor in the observed period. We also observed strong treatment effects in xenograft models which are comparable to results shown in preclinical approaches using melanoma-specific CAR T cells.^{33–36} In these studies, HER2 and GD2 were the targeted antigens. HER2 CAR T cells have been shown to pose a risk of lethal toxicity, with cytokine release syndrome from on-target off-tumor recognition of HER2.³⁷ While efforts are being made to create safer HER2-targeting CAR T cells,³⁸ we demonstrate herein that the SAR T cell-BiAb approach, with its controllable and reversible facets, can be a ready-made solution for lowering and controlling toxicity.³⁹

MCSP is differentially expressed on the surface of over 85% of melanomas.⁴⁰ It provides tumorigenic signals to melanoma cells that stimulate growth, motility, and tissue invasion.^{41–44} It was therefore unsurprising to discover its expression was retained on patient with primary melanoma samples irrespective of the treatment history. Furthermore, we could show expression on human melanoma cell lines on transcript and protein level which was in line with the functional readouts. MCSP has been described as potential target for CAR T cell therapy in melanoma and glioblastoma.^{39, 45} TYRP1, a transmembrane glycoprotein naturally involved in melanin production,⁴⁶ has been identified as an antigen highly expressed in melanoma and stably expressed during disease progression.⁴⁷ TYRP1 expression could also be observed on primary patient samples and human melanoma cell lines. Discrepancies between transcript and protein expression could be partly caused by internalization of TYRP1.^{48, 49} The influence of target antigen internalization on treatment outcome must be investigated in further studies. Nonetheless, potent treatment effects were shown when targeting TYRP1⁺ cells with the SAR-BiAb approach in syngeneic and human xenograft models. In a phase I study an anti-TYRP1 monoclonal antibody was administered in patients with relapsed or refractory melanoma, where no serious adverse events were observed, indicating the potential safety of targeting.⁵⁰

With low off-tumor expression detected in some healthy tissues for both targets, it was necessary to design antibodies that would bind MCSP and TYRP1 with sufficient avidity, while minimizing the potential for off-tumor toxicity. Melanoma-specific BiAb were designed with two binding arms for the tumor target. This increased the binding avidity of the BiAb to melanoma cells showing higher target expression compared with healthy cells. Thus, the binding strength could be increased while minimizing the risk of on-target off-tumor toxicity that is often associated with increased binding affinities. Similarly, the risk of targeting endogenous T cells is limited since no expression of the target antigens was observed on human T cells. The modular facets of the SAR platform were

previously demonstrated in an acute myeloid leukemia xenograft model,¹⁹ and again substantiated herein. The simultaneous, or in the event of antigen loss, sequential targeting of multiple tumor antigens has proven to be an effective approach in the treatment of B-cell malignancies,⁵¹ and is further evidenced by several approaches attempting to render CAR T cells more adaptable.⁵² We thereby reason, that a platform allowing change or simultaneous targeting of multiple antigens, with one cellular construct comes with clear advantages of feasibility and flexibility.

MCSP levels have been shown to be elevated in the sera of patients with advanced melanoma.³² We experimentally tested the potential impact of soluble MCSP on the conditional specificity of the SAR T cell-BiAb approach. At physiological levels, free-MCSP did not activate SAR T cells in the presence of BiAb. Free targeted protein in the tumor microenvironment must be considered as a potential hindrance to the efficacy of the SAR T cell-BiAb combination, as well as other adoptive T cell therapies. This could become especially problematic in targeting cleavable proteins, such as MCSP, and the targeting of membrane-associated forms of proteins could maximize efficiency in this regard.³² In fact, shed glypican-3 was shown to induce a blocking effect on CAR T cells targeting glypican-3-expressing hepatocellular carcinoma.⁵³ Probably because of the peculiarities of the SAR T cell-BiAb platform, we have not found such mechanism to impact efficacy or activity.

Anti-melanoma CAR T cell therapy has shown limited efficacy in the clinic thus far.⁵⁴ Results from the CARPETS phase I trial (NCT02107963) showed limited persistence of GD2 CAR T cells in patients with metastatic melanoma, with CAR transgenes only detected at low levels in patient peripheral blood after 4 months. T cell exhaustion and activation induced cell death have been shown to hinder the persistence and function of adoptively transferred T cells.^{55,56} Recent work from Weber and colleagues showed that transient rest, using enforced CAR molecule downregulation via a drug-regulatable system, could restore CAR T cell functionality.⁵⁷ An advantage of the SAR T cell-BiAb system is that it is an adaptor platform inherently regulatable, via its BiAb facet. The reversibility of SAR T cell activation was demonstrated with the cessation of BiAb dosing in vitro and in vivo. This makes it very straightforward to incorporate a transient rest period simply by modifying the dosing schedule of the BiAb, thus recapitulating the previously mentioned regulatable system. Recent work by Phillipp and colleagues also showed that transient BiAb dosing reduced T cell exhaustion and improved CD3⁺ T cell engager efficacy.⁵⁸ The BiAb molecules we used have an IgG format, which extends their half-life in comparison to Fc-deficient BiAb.⁵⁹ Engineering the half-life of BiAb to offer greater flexibility towards patient needs would be a straightforward approach, that could also be beneficial. Importantly, we could previously demonstrate the use of different antibody formats and half-lives to activate and redirect SAR T cells,^{19,20} opening the door to

such optimizations. Inadequate T cell infiltration into the tumor and a suppressive milieu therein are the subject of ongoing investigation that could broadly improve the therapeutic success of adoptive T cell therapies in solid tumors,⁵ including melanoma. Equipping SAR T cells with relevant chemokine receptors while shielding them from local immune suppression could further improve treatment efficacy and warrant further investigation.^{24,26}

Harnessing the apparent advantages of the SAR T cell-BiAb platform for melanoma therapy has yielded very promising results in our preclinical models. With evident potential for improved clinical benefit, we believe these findings warrant further characterization in more advanced preclinical models and ultimately clinical studies.

Author affiliations

¹Department of Medicine IV, Division of Clinical Pharmacology, Klinikum der Universität München, Munich, Germany

²Roche Innovation Center Zurich, Roche Pharma Research & Early Development, Schlieren, Switzerland

³Department of Medicine III, Klinikum der Universität München, Munich, Germany

⁴German Cancer Consortium (DKTK), Partner Site Munich, Munich, Germany

⁵Institute of AI for Health, Helmholtz Center Munich, German Research Center for Environmental Health, Neuherberg, Germany

⁶Institute of Computational Biology, Helmholtz Center Munich, German Research Center for Environmental Health, Neuherberg, Germany

⁷School of Life Sciences Weihenstephan, Technical University of Munich, Munich, Freising, Germany

⁸Division of Pediatric Nephrology, Department of Pediatrics, Dr. v. Haunersches Kinderspital, Klinikum der Universität München, Munich, Germany

⁹Department of Dermatology, University Hospital Zurich, Schlieren, Switzerland

¹⁰Department of Dermatology, Universitätsklinikum Erlangen, Friedrich-Alexander Universität Erlangen-Nürnberg (FAU), Erlangen, Germany

¹¹Deutsches Zentrum Immuntherapie (DZI), Friedrich-Alexander-Universität Erlangen-Nürnberg, Erlangen, Germany

¹²Einheit für Klinische Pharmakologie (EKLiP), Helmholtz Center Munich, German Research Center for Environmental Health, Neuherberg, Germany

Twitter Mohamed-Reda Benmebarek @MRbenmebarek, Julius Keyl @JuliusKeyl, Bruno L Cadilha @bcadilha and Sophia Stock @SophiaStock_

Acknowledgements The authors acknowledge the Core Facility Flow Cytometry of the University Hospital, LMU Munich, for assistance with the generation of flow cytometry data. Figure 4C was created with BioRender.com. SS was supported by the Else Kröner-Fresenius Clinician Scientist Program Cancer Immunotherapy, the Munich Clinician Scientist Program (MCSP) and the DKTK School of Oncology. SM, JJ, MS, A-KK, TL and RK were supported by a grant from the Förderprogramm für Forschung und Lehre (FöFoLe) of the Ludwig Maximilian University (LMU) of Munich.

Contributors Conceptualization: M-RB, FM, CK and SK. Methodology: FM, M-RB, DB, PJM, JJ, MT, JK, LM, CK and MS. Investigation: M-RB, FM, HO and MT. Validation: HO, MS, A-KK, TL, SS, SM and RG. Writing—original draft: M-RB and FM. Writing—review and editing: M-RB, FM, BLC, JK, MG, MS, MT, MVH, SE, CK and SK. Funding acquisition: SE and SK. Resources: DB, AG, CM, SR, MPL, MVH, SE, CK and SK. Supervision: RK, CM and SK. Guarantor: M-RB and FM.

Funding The in vivo imaging device was funded by the Deutsche Forschungsgemeinschaft (DFG, German Research Foundation) – INST 409/231-1. MT is funded by the Volkswagen Foundation (project OntoTime). CM has received funding from the European Research Council (ERC) under the European Union's Horizon 2020 research and innovation programme (grant agreement number 866411). This study was supported by the Marie-Sklodowska-Curie Program Training Network for Optimizing Adoptive T Cell Therapy of Cancer funded by the H2020 Program of the European Union (Grant 955575, to SK); by the Hector Foundation (to SK); by the International Doctoral Program i-Target: Immunotargeting of Cancer funded by the Elite Network of Bavaria (to SK and SE); by Melanoma Research Alliance Grants 409510 (to SK); by the Else Kröner-Fresenius-Stiftung (to SK and RK); by the German Cancer Aid (to SK); by the Ernst-Jung-Stiftung (to

SK); by the LMU Munich's Institutional Strategy LMUexcellent within the framework of the German Excellence Initiative (to SE and SK); by the Go-Bio initiative (to SK); by the m4 Award of the Bavarian Ministry of Economical Affairs, by the Bundesministerium für Bildung und Forschung (SK); by the European Research Council Grant 756017, ARMOR-T (to SK) and the ERC proof-of-concept Grant 101100460 (to SK); by the Deutsche Forschungsgemeinschaft (DFG, German Research Foundation) (KO5055-2-1 and 510821390 to SK); by the SFB-TRR 338/1 2021–452881907 (to SK); by the Wilhelm-Sander-Stiftung, by the Fritz-Bender Foundation (to SK) and by the Deutsche José-Carreras Leukämie Stiftung (to SK).

Competing interests Parts of this work were performed in partial fulfillment of the requirements of the Munich Medical Research School for doctoral graduation of FM. SK has received honoraria from TCR2 Miltenyi Biotec, Novartis, BMS and GSK. SK and SE are inventors of several patents in the field of immuno-oncology. SK and SE received license fees from TCR2 and Carina Biotech. SK and SE received research support from TCR2, Arcus Bioscience, Plectonic GmbH and Tabby Therapeutics for work unrelated to the manuscript. MG and CK declare employment, patents and stock ownership with Roche.

Patient consent for publication Not applicable.

Ethics approval Written informed consent was obtained from all patients after approval by the local committees of the Klinikum der Universität München and the Cantonal Ethics Committee of Zürich.

Provenance and peer review Not commissioned; externally peer reviewed.

Data availability statement Data are available upon reasonable request. Data supporting this manuscript is attached. Raw data and reagents will be made available upon reasonable request to the authors.

Supplemental material This content has been supplied by the author(s). It has not been vetted by BMJ Publishing Group Limited (BMJ) and may not have been peer-reviewed. Any opinions or recommendations discussed are solely those of the author(s) and are not endorsed by BMJ. BMJ disclaims all liability and responsibility arising from any reliance placed on the content. Where the content includes any translated material, BMJ does not warrant the accuracy and reliability of the translations (including but not limited to local regulations, clinical guidelines, terminology, drug names and drug dosages), and is not responsible for any error and/or omissions arising from translation and adaptation or otherwise.

Open access This is an open access article distributed in accordance with the Creative Commons Attribution Non Commercial (CC BY-NC 4.0) license, which permits others to distribute, remix, adapt, build upon this work non-commercially, and license their derivative works on different terms, provided the original work is properly cited, appropriate credit is given, any changes made indicated, and the use is non-commercial. See <http://creativecommons.org/licenses/by-nc/4.0/>.

ORCID iDs

Florian Märkl <http://orcid.org/0000-0003-4285-0380>

Mohamed-Reda Benmehbarek <http://orcid.org/0000-0002-1201-7067>

Sophia Stock <http://orcid.org/0000-0002-5072-5013>

Matthias Seifert <http://orcid.org/0000-0002-6581-6196>

Theo Lorenzini <http://orcid.org/0000-0003-3377-032X>

Ruth Grünmeier <http://orcid.org/0000-0002-9044-3600>

Moritz Thomas <http://orcid.org/0000-0002-8422-2414>

Stefan Endres <http://orcid.org/0000-0002-4703-537X>

Christian Klein <http://orcid.org/0000-0001-7594-7280>

Sebastian Kobold <http://orcid.org/0000-0002-5612-4673>

REFERENCES

- Hodis E, Watson IR, Kryukov GV, *et al.* A landscape of driver mutations in melanoma. *Cell* 2012;150:251–63.
- Cohen CJ, Gartner JJ, Horovitz-Fried M, *et al.* Isolation of neoantigen-specific T cells from tumor and peripheral lymphocytes. *J Clin Invest* 2015;125:3981–91.
- Blank CU, Rozeman EA, Fanchi LF, *et al.* Neoadjuvant versus adjuvant ipilimumab plus nivolumab in macroscopic stage III melanoma. *Nat Med* 2018;24:1655–61. 10.1038/s41591-018-0198-0
- Larkin J, Chiarion-Sileni V, Gonzalez R, *et al.* Five-Year survival with combined nivolumab and ipilimumab in advanced melanoma. *N Engl J Med* 2019;381:1535–46.
- Lesch S, Benmehbarek M-R, Cadilha BL, *et al.* Determinants of response and resistance to CAR T cell therapy. *Semin Cancer Biol* 2020;65:80–90.
- Maibach F, Sadozai H, Seyed Jafari SM, *et al.* Tumor-Infiltrating lymphocytes and their prognostic value in cutaneous melanoma. *Front Immunol* 2020;11:2105.
- Rosenberg SA, Packard BS, Aebbersold PM, *et al.* Use of tumor-infiltrating lymphocytes and interleukin-2 in the immunotherapy of patients with metastatic melanoma. *N Engl J Med* 1988;319:1676–80.
- Hont AB, Cruz CR, Ulrey R, *et al.* Immunotherapy of relapsed and refractory solid tumors with ex vivo expanded multi-tumor associated antigen specific cytotoxic T lymphocytes: a phase I study. *J Clin Oncol* 2019;37:2349–59.
- Chandran SS, Klebanoff CA. T cell receptor-based cancer immunotherapy: emerging efficacy and pathways of resistance. *Immunol Rev* 2019;290:127–47.
- Borch TH, Andersen R, Ellebaek E, *et al.* Future role for adoptive T-cell therapy in checkpoint inhibitor-resistant metastatic melanoma. *J Immunother Cancer* 2020;8:e000668.
- Sim GC, Chacon J, Haymaker C, *et al.* Tumor-Infiltrating lymphocyte therapy for melanoma: rationale and issues for further clinical development. *BioDrugs* 2014;28:421–37.
- June CH, O'Connor RS, Kawalekar OU, *et al.* Car T cell immunotherapy for human cancer. *Science* 2018;359:1361–5.
- Neelapu SS, Locke FL, Bartlett NL, *et al.* Axicabtagene ciloleucel CAR T-cell therapy in refractory large B-cell lymphoma. *N Engl J Med* 2017;377:2531–44.
- Hill JA, Giral S, Torgerson TR, *et al.* CAR-T and a side order of IgG, to go? -immunoglobulin replacement in patients receiving CAR-T cell therapy. *Blood Rev* 2019;38:S0268-960X(19)30067-0.
- Beatty GL, O'Hara MH, Lacey SF, *et al.* Activity of mesothelin-specific chimeric antigen receptor T cells against pancreatic carcinoma metastases in a phase 1 trial. *Gastroenterology* 2018;155:29–32.
- Khong HT, Wang QJ, Rosenberg SA. Identification of multiple antigens recognized by tumor-infiltrating lymphocytes from a single patient: tumor escape by antigen loss and loss of MHC expression. *J Immunother* 2004;27:184–90.
- Rataj F, Jacobi SJ, Stoiber S, *et al.* High-Affinity CD16-polymorphism and fc-engineered antibodies enable activity of CD16-chimeric antigen receptor-modified T cells for cancer therapy. *Br J Cancer* 2019;120:79–87.
- Stock S, Benmehbarek M-R, Kluever A-K, *et al.* Chimeric antigen receptor T cells engineered to recognize the P329G-mutated Fc part of effector-silenced tumor antigen-targeting human IgG1 antibodies enable modular targeting of solid tumors. *J Immunother Cancer* 2022;10:e005054.
- Benmehbarek M-R, Cadilha BL, Herrmann M, *et al.* A modular and controllable T cell therapy platform for acute myeloid leukemia. *Leukemia* 2021;35:2243–57.
- Karches CH, Benmehbarek M-R, Schmidbauer ML, *et al.* Bispecific antibodies enable synthetic agonistic receptor-transduced T cells for tumor immunotherapy. *Clin Cancer Res* 2019;25:5890–900.
- Schaefer W, Regula JT, Böhner M, *et al.* Immunoglobulin domain crossover as a generic approach for the production of bispecific IgG antibodies. *Proc Natl Acad Sci U S A* 2011;108:11187–92.
- Surowka M, Schaefer W, Klein C. Ten years in the making: application of crossmab technology for the development of therapeutic bispecific antibodies and antibody fusion proteins. *MAbs* 2021;13:1967714.
- Ghani K, Wang X, de Campos-Lima PO, *et al.* Efficient human hematopoietic cell transduction using RD114- and GALV-pseudotyped retroviral vectors produced in suspension and serum-free media. *Hum Gene Ther* 2009;20:966–74.
- Lesch S, Blumenberg V, Stoiber S, *et al.* T cells armed with C-X-C chemokine receptor type 6 enhance adoptive cell therapy for pancreatic tumours. *Nat Biomed Eng* 2021;5:1246–60.
- Carter P, Presta L, Gorman CM, *et al.* Humanization of an anti-1B5HER2 antibody for human cancer therapy. *Proc Natl Acad Sci U S A* 1992;89:4285–9.
- Cadilha BL, Benmehbarek M-R, Dorman K, *et al.* Combined tumor-directed recruitment and protection from immune suppression enable CAR T cell efficacy in solid tumors. *Sci Adv* 2021;7:eabi5781.
- Kobold S, Grassmann S, Chaloupka M, *et al.* Impact of a new fusion receptor on PD-1-mediated immunosuppression in adoptive T cell therapy. *J Natl Cancer Inst* 2015;107:djv146.
- Journe F, Id Boufker H, Van Kempen L, *et al.* Tymp1 mRNA expression in melanoma metastases correlates with clinical outcome. *Br J Cancer* 2011;105:1726–32.
- Erfurt C, Sun Z, Haendle I, *et al.* Tumor-reactive CD4+ T cell responses to the melanoma-associated chondroitin sulphate proteoglycan in melanoma patients and healthy individuals in the absence of autoimmunity. *J Immunol* 2007;178:7703–9.

- 30 Pérez-Lorenzo R, Erjavec SO, Christiano AM, *et al.* Improved therapeutic efficacy of unmodified anti-tumor antibodies by immune checkpoint blockade and kinase targeted therapy in mouse models of melanoma. *Oncotarget* 2021;12:66–80.
- 31 Tirosh I, Izar B, Prakadan SM, *et al.* Dissecting the multicellular ecosystem of metastatic melanoma by single-cell RNA-seq. *Science* 2016;352:189–96.
- 32 Vergilis IJ, Szarek M, Ferrone S, *et al.* Presence and prognostic significance of melanoma-associated antigens CYT-MAA and HMW-MAA in serum of patients with melanoma. *J Invest Dermatol* 2005;125:526–31.
- 33 Forsberg EMV, Lindberg MF, Jespersen H, *et al.* Her2 CAR-T cells eradicate uveal melanoma and T-cell therapy-resistant human melanoma in IL2 transgenic NOD/SCID IL2 receptor knockout mice. *Cancer Res* 2019;79:899–904.
- 34 Yu J, Wu X, Yan J, *et al.* Anti-GD2/4-1BB chimeric antigen receptor T cell therapy for the treatment of Chinese melanoma patients. *J Hematol Oncol* 2018;11:1.
- 35 Beard RE, Zheng Z, Lagisetty KH, *et al.* Multiple chimeric antigen receptors successfully target chondroitin sulfate proteoglycan 4 in several different cancer histologies and cancer stem cells. *J Immunother Cancer* 2014;2:25.
- 36 Geldres C, Savoldo B, Hoyos V, *et al.* T lymphocytes redirected against the chondroitin sulfate proteoglycan-4 control the growth of multiple solid tumors both in vitro and in vivo. *Clin Cancer Res* 2014;20:962–71.
- 37 Morgan RA, Yang JC, Kitano M, *et al.* Case report of a serious adverse event following the administration of T cells transduced with a chimeric antigen receptor recognizing ErbB2. *Molecular Therapy* 2010;18:843–51.
- 38 Liu X, Zhang N, Shi H. Driving better and safer HER2-specific cars for cancer therapy. *Oncotarget* 2017;8:62730–41.
- 39 Wang Y, Geldres C, Ferrone S, *et al.* Chondroitin sulfate proteoglycan 4 as a target for chimeric antigen receptor-based T-cell immunotherapy of solid tumors. *Expert Opin Ther Targets* 2015;19:1339–50.
- 40 Campoli MR, Chang C-C, Kageshita T, *et al.* Human high molecular weight-melanoma-associated antigen (HMW-MAA): a melanoma cell surface chondroitin sulfate proteoglycan (MSCP) with biological and clinical significance. *Crit Rev Immunol* 2004;24:267–96.
- 41 Eisenmann KM, McCarthy JB, Simpson MA, *et al.* Melanoma chondroitin sulphate proteoglycan regulates cell spreading through Cdc42, Ack-1 and p130Cas. *Nat Cell Biol* 1999;1:507–13.
- 42 Yang X, Kovalenko OV, Tang W, *et al.* Palmitoylation supports assembly and function of integrin-tetraspanin complexes. *J Cell Biol* 2004;167:1231–40.
- 43 Yang J, Price MA, Li GY, *et al.* Melanoma proteoglycan modifies gene expression to stimulate tumor cell motility, growth, and epithelial-to-mesenchymal transition. *Cancer Res* 2009;69:7538–47.
- 44 Iida J, Wilhelmson KL, Ng J, *et al.* Cell surface chondroitin sulfate glycosaminoglycan in melanoma: role in the activation of pro-MMP-2 (pro-gelatinase A). *Biochem J* 2007;403:553–63.
- 45 Pellegatta S, Savoldo B, Di Ianni N, *et al.* Constitutive and TNF α -inducible expression of chondroitin sulfate proteoglycan 4 in glioblastoma and neurospheres: implications for CAR-T cell therapy. *Sci Transl Med* 2018;10:430.
- 46 Ghanem G, Fabrice J. Tyrosinase related protein 1 (TYRP1/gp75) in human cutaneous melanoma. *Mol Oncol* 2011;5:150–5.
- 47 Asgarov K, Balland J, Tirole C, *et al.* A new anti-mesothelin antibody targets selectively the membrane-associated form. *MAbs* 2017;9:567–77.
- 48 Bultema JJ, Boyle JA, Malenke PB, *et al.* Myosin Vc interacts with Rab32 and Rab38 proteins and works in the biogenesis and secretion of melanosomes. *J Biol Chem* 2014;289:33513–28.
- 49 Truschel ST, Simoes S, Setty SRG, *et al.* Escrt-I function is required for TYRP1 transport from early endosomes to the melanosome limiting membrane. *Traffic* 2009;10:1318–36.
- 50 Khalil DN, Postow MA, Ibrahim N, *et al.* An open-label, dose-escalation phase I study of Anti-TYRP1 monoclonal antibody IMC-20D7S for patients with relapsed or refractory melanoma. *Clin Cancer Res* 2016;22:5204–10.
- 51 Spiegel JY, Patel S, Muffly L, *et al.* CAR T cells with dual targeting of CD19 and CD22 in adult patients with recurrent or refractory B cell malignancies: a phase 1 trial. *Nat Med* 2021;27:1419–31.
- 52 Darowski D, Kobold S, Jost C, *et al.* Combining the best of two worlds: highly flexible chimeric antigen receptor adaptor molecules (CAR-adaptors) for the recruitment of chimeric antigen receptor T cells. *MAbs* 2019;11:621–31.
- 53 Sun L, Gao F, Gao Z, *et al.* Shed antigen-induced blocking effect on CAR-T cells targeting glypican-3 in hepatocellular carcinoma. *J Immunother Cancer* 2021;9:e001875.
- 54 Gargett T, Yu W, Dotti G, *et al.* GD2-specific CAR T cells undergo potent activation and deletion following antigen encounter but can be protected from activation-induced cell death by PD-1 blockade. *Mol Ther* 2016;24:1135–49.
- 55 Long AH, Haso WM, Shern JF, *et al.* 4-1Bb costimulation ameliorates T cell exhaustion induced by tonic signaling of chimeric antigen receptors. *Nat Med* 2015;21:581–90.
- 56 Stoiber S, Cadilha BL, Benmehar M-R, *et al.* Limitations in the design of chimeric antigen receptors for cancer therapy. *Cells* 2019;8:472.
- 57 Weber EW, Parker KR, Sotillo E, *et al.* Transient rest restores functionality in exhausted CAR-T cells through epigenetic remodeling. *Science* 2021;372:6537.
- 58 Philipp N, Kazerani M, Nicholls A, *et al.* T-cell exhaustion induced by continuous bispecific molecule exposure is ameliorated by treatment-free intervals. *Blood* 2022;140:1104–18.
- 59 Labrijn AF, Janmaat ML, Reichert JM, *et al.* Bispecific antibodies: a mechanistic review of the pipeline. *Nat Rev Drug Discov* 2019;18:585–608.

BiAb redirect SAR T cell therapy in melanoma**1 SUPPLEMENTARY METHODS****2 Processing and analysis of single-cell RNA-sequencing data**

3 All analyses from UMI count matrices were run with python 3 with the Scanpy API v.1.4.6¹ and
4 anndata v.0.7.1.² to obtain high quality cells, barcodes from GSE72056 were filtered based on
5 total UMI counts and total genes after visual inspection of distributions. Cells with over 20000
6 counts or 10000 genes as well as cells with under 6000 counts or 2000 genes were removed.
7 Genes with expression in less than 20 cells were excluded. Cells were normalised using the
8 SCRAN algorithm,³ expression values were then log-transformed. The top 4000 highly variable
9 genes were selected based on normalised dispersion as described in.⁴ To efficiently capture the
10 underlying data structure in two dimensions, a neighborhood graph was computed on the first
11 50 principal components using Scanpy's pp.neighbors with 15 neighbors. For 2D visualization,
12 embedding the neighborhood graph via UMAP was done by running Scanpy's tl.umap with
13 default parameters. Annotations of cells were provided by the authors.

14 Analysis of TYRP1 and MCSP expression using flow cytometry

15 Cells were detached using Accutase solution (Capricorn Scientific). Dead cells were stained
16 using the eFluor™ 780 fixable viability dye (1:1000, eBioscience, Thermo Fisher Scientific) for
17 15 minutes at room temperature, followed by staining of cell surface proteins using either 0.5
18 µg/mL of αMCSP/αE3 at 4°C or αTYRP1/αE3 at 37 °C for 30 minutes. Then, staining of primary
19 antibodies were conducted using a secondary goat polyclonal antibody against human IgG (2.5
20 µg/mL, Southern Biotech) for 15 minutes at room temperature. Median fluorescence intensity
21 (MFI) ratio was calculated based on ratio of MCSP or TYRP1 stain and secondary antibody only
22 stain.

Cells were analyzed on LSRFortessa (BD Biosciences) or CytoFLEX (Beckman Coulter Life Sciences) flow cytometers, and data were analyzed with FlowJo software version 9.9.5 or version 10.3.

Analysis of TYRP1 and MCSP expression using confocal microscopy

Cells were detached using Accutase solution (Capricorn Scientific), transferred to Poly-L-Lysine coated SuperFrost Plus slides (Thermo Fisher Scientific) and incubated at 37 °C for 60 minutes for cell attachment. Cells were first fixed with 1 % PFA solution (Carl Roth) for 10 minutes and washed with PBS. For TYRP1 staining cells were permeabilized with Triton X100 (v/v 0,5%, Carl Roth). Following permeabilization cells were stained with 1 µg/mL αTYRP1/αE3 for 60 minutes at room temperature. MCSP staining of non-permeabilized cells was conducted with 10 µg/mL αMCSP/αE3 for 60 minutes at room temperature. Then, secondary antibody against human IgG (1 µg/mL, Southern Biotech) and DNA dye Hoechst 33342 (2 µM, Thermo Fisher Scientific) were applied for 30 minutes at room temperature. After sealing cells with ProLong Glass antifade mountant (Thermo Fisher Scientific), samples were analyzed using the laser-scanning confocal microscope ZEISS LSM 800 (Carl Zeiss AG) and images were acquired using Zen software (v2.3, Carl Zeiss AG).

Preparation of single cell suspensions, antibody staining and flow cytometry

Lymph nodes and spleens were passed through 30 µm cell strainers, followed by erythrocyte lysis in the spleens. Tumors and lungs were digested with 1.5 mg/mL collagenase IV and 50 U/mL DNase I for 30 minutes at 37 °C under agitation. Dead cells were stained using the violet fixable viability dye (BioLegend) for 15 minutes at room temperature, followed by blocking of Fc receptors with TruStain FcX (BioLegend) for 20 minutes at 4 °C. Following this, cell surface proteins were stained for 20 minutes at 4 °C. For the analysis of human T cells antibodies against CD45 (2D1), CD3 (OKT3), CD4 (OKT4) CD8a (RPA-T8), CD45RO (UCHL1),

BiAb redirect SAR T cell therapy in melanoma

47 CCR7 (G043H7), PD-1 (EH12.2H7), 4-1BB (4B4-1), CD69 (FN50) and EGFR (A-13) for
48 detection of SAR (all from BioLegend) were used. For the analysis of murine T cells antibodies
49 against CD45 (30-F11), CD3 (17a2), CD4 (GK1.5) CD8a (53-6.7) and EGFR (A-13) for
50 detection of SAR (all from BioLegend) were used. Additionally, tumor cells were detected using
51 the GFP expression of YUMM1.1 TYRP1-LUC-GFP cells.

52 Cells were analyzed on Canto or LSRFortessa flow cytometers (BD Biosciences), and data
53 were analyzed with FlowJo software version 9.9.5 or version 10.3.

54 Construction of 2 + 1 bispecific antibodies

55 The construction of expression vectors for BiAb was performed by standard recombinant DNA
56 technologies. All antibody chain genes were separately inserted into expression vectors under
57 control of a MPSV or a SV40E hCMV promoter. The plasmids were cotransfected and
58 transiently expressed in HEK293 or CHO cells. The 2 + 1 antibody contained two Fabs for
59 hMCSP or TYRP1 and one Fab for EGFRvIII which was N-terminally fused to one arm of the
60 hMCSP or TYRP1 IgG. In order to obtain high yields of correctly paired molecules the "knobs-
61 into-holes" technology was used for heterodimerization. P329G, L234A, and L235A (PG LALA)
62 mutations were inserted in CH3 and CH2 domains to prevent binding to FcγRs and C1q.^{5 6} To
63 ensure correct pairing of the different chains, the CrossMAb^{VH-VL} technology (αEGFRvIII) and
64 charged residues (αMCSP) were used.⁷

65 Purification and quality control

66 All antibodies were transiently produced in HEK293 or CHO cells, purified and analyzed for
67 integrity and monomer content, as previously described.⁵

68 Bispecific antibody binding assays

69 Apparent dissociation constants (K_D) were measured by calibrated flow cytometry on a Fortessa
70 II instrument (BD Biosciences) with 3.0 to 3.4 μm Rainbow Calibration particles (BioLegend) as
71 calibration control.⁸ After normalization, data points were fitted to a one-site specific binding
72 model.

73
74 **Supplementary Table 1: Patient characteristics**

Name / cells	Biopsy	Patient age at biopsy time	Gender	Clinical stage at biopsy time	Site of biopsy	Tx before biopsy	Tx after biopsy	Primary tumor subtype	Primary tumor location	Breslow's index of primary tumor	Genotype
Patient 1	n. a.	n. a.	n. a.	n. a.	n. a.	n. a.	n. a.	n. a.	n. a.	n. a.	n. a.
Patient 2	n. a.	n. a.	n. a.	n. a.	n. a.	n. a.	n. a.	n. a.	n. a.	n. a.	n. a.
Patient 3	n. a.	n. a.	n. a.	n. a.	n. a.	n. a.	n. a.	n. a.	n. a.	n. a.	n. a.
Patient 4	n. a.	n. a.	n. a.	n. a.	n. a.	n. a.	n. a.	n. a.	n. a.	n. a.	n. a.
Patient 5	n. a.	n. a.	n. a.	n. a.	n. a.	n. a.	n. a.	n. a.	n. a.	n. a.	n. a.
Patient 6	n. a.	n. a.	n. a.	n. a.	n. a.	n. a.	n. a.	n. a.	n. a.	n. a.	n. a.
Patient 7	n. a.	n. a.	n. a.	n. a.	n. a.	n. a.	n. a.	n. a.	n. a.	n. a.	n. a.
Patient 8	Metastasis (skin)	61 yo	Female	III	Skin (leg)	Dabrafenib (BRAF) and trametinib (MEK)	Ipilimumab; Encorafenib (BRAF) + Binimetinib (MEK) + Infigratinib (FGFR); Pembrolizumab; radiation therapy (30Gy); multiple excisions; electro-chemotherapy (bleomycin); vemurafenib; TVEC	Nodular melanoma	Leg	4 mm	BRAF V600E, NRASwt
Patient 9	Metastasis (skin)	n. a.	n. a.	n. a.	Skin	n. a.	n. a.	n. a.	n. a.	n. a.	n. a.
Patient 10	Metastasis (skin)	n. a.	n. a.	n. a.	Skin	n. a.	n. a.	n. a.	n. a.	n. a.	n. a.
Patient 11	Primary melanoma	73 yo	Male	IV	Skin (abdomen)	None	Transarterial chemoembolization (patient was also diagnosed with hepatocellular carcinoma 2 months later)	Nodular melanoma with ulceration mitotic index 5/mm ² T3b	Abdomen	4 mm	n. a.
Patient 12	Primary melanoma	86 yo	Female	III	Skin (neck)	None	n. a.	Nodular melanoma	Neck	n. a.	n. a.
Patient 13	Metastasis (brain)	36 yo	Female	IV	Brain	None	None	n. a.	Forehead	3 mm	BRAF V600

75
76
77
78
79
80

81 **REFERENCES**

BiAb redirect SAR T cell therapy in melanoma

1. Wolf FA, Angerer P, Theis FJ. SCANPY: large-scale single-cell gene expression data analysis. *Genome Biology* 2018;19(1):15. doi: 10.1186/s13059-017-1382-0
2. Virshup I, Rybakov S, Theis FJ, et al. anndata: Annotated data. *bioRxiv* 2021:2021.12.16.473007. doi: 10.1101/2021.12.16.473007
3. Lun AT, Bach K, Marioni JC. Pooling across cells to normalize single-cell RNA sequencing data with many zero counts. *Genome Biology* 2016;17(1):75. doi: 10.1186/s13059-016-0947-7
4. Zheng GX, Terry JM, Belgrader P, et al. Massively parallel digital transcriptional profiling of single cells. *Nat Commun* 2017;8:14049. doi: 10.1038/ncomms14049 [published Online First: 20170116]
5. Karches CH, Benmeharek M-R, Schmidbauer ML, et al. Bispecific Antibodies Enable Synthetic Agonistic Receptor-Transduced T Cells for Tumor Immunotherapy. *Clinical Cancer Research* 2019;25(19):5890-900. doi: 10.1158/1078-0432.Ccr-18-3927
6. Hessel AJ, Hangartner L, Hunter M, et al. Fc receptor but not complement binding is important in antibody protection against HIV. *Nature* 2007;449(7158):101-4. doi: 10.1038/nature06106
7. Schaefer W, Regula JT, Böhner M, et al. Immunoglobulin domain crossover as a generic approach for the production of bispecific IgG antibodies. *Proceedings of the National Academy of Sciences* 2011;108(27):11187-92. doi: 10.1073/pnas.1019002108
8. Benedict CA, MacKrell AJ, Anderson WF. Determination of the binding affinity of an anti-CD34 single-chain antibody using a novel, flow cytometry based assay. *Journal of Immunological Methods* 1997;201(2):223-31. doi: [https://doi.org/10.1016/S0022-1759\(96\)00227-X](https://doi.org/10.1016/S0022-1759(96)00227-X)

A

Patient 1: 27.5, 9.77
Patient 2: 2.00, 1.73
Patient 3: 2.32, 2.30
Patient 4: 6.95, 3.22
Patient 5: 37.4, 1.61
Patient 6: 4.81, 1.16
PANC-1: 1.07, 1.08
Patient 8: 27.7, 1.11
Patient 9: 2.52, 1.50
Patient 10: 2.81, 1.98
Patient 11: 13.0, 1.47
Patient 12: 5.96, 1.22
A375: 2.84, 1.27
MV3: 6.84, 2.46
human T cells: 0.94, 0.82

— Secondary antibody only
— MCSP stain
— TYRP1 stain

B

αTyrP1 structure diagram showing domains: VH, VL, CH1, Ck, CH2, CH3. Mutations: PG LALA mutations in CH2 and CH3, „Knobs-into-holes“ in CH3.

C

αTyrP1 structure diagram showing domains: VH, VL, CH1, Ck, CH2, CH3. Mutations: PG LALA mutations in CH2 and CH3, „Knobs-into-holes“ in CH3.

D

MFI of αTyrP1/αE3 on YUMM1.1 cells binding vs µg/mL

E

MFI of αTyrP1/αE3 on YUMM1.1 cells binding vs µg/mL

F

MFI of αTyrP1/αE3 on YUMM1.1 cells binding vs µg/mL

G

TYRP1 gene expression normalised to β-actin

YUMM1.1, YUMM1.1 TYRP1, B16, Panc02-Ova, murine T cells

H

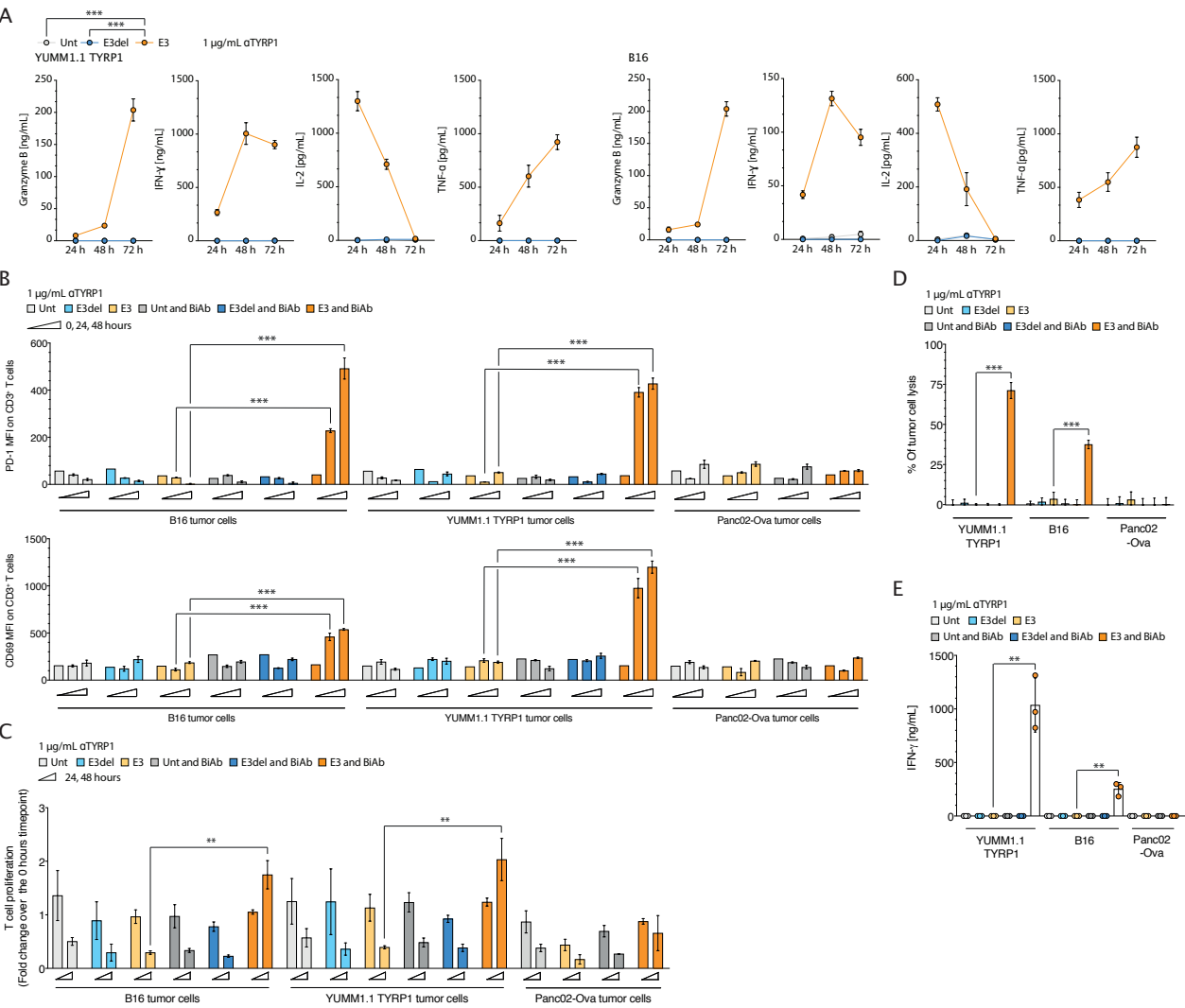
YUMM1.1: 1.08, 5.82
YUMM1.1 TYRP1: 148, 0.97
B16: 0.96

— Secondary antibody only
— TYRP1 stain

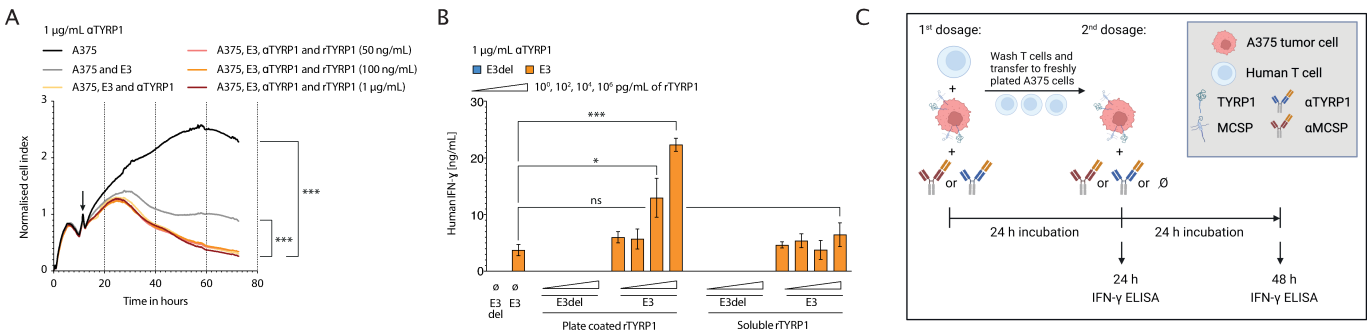
I

Immunofluorescence images of YUMM1.1, B16, and Panc02-Ova cells stained with αTyrP1 (red) and DAPI (blue).

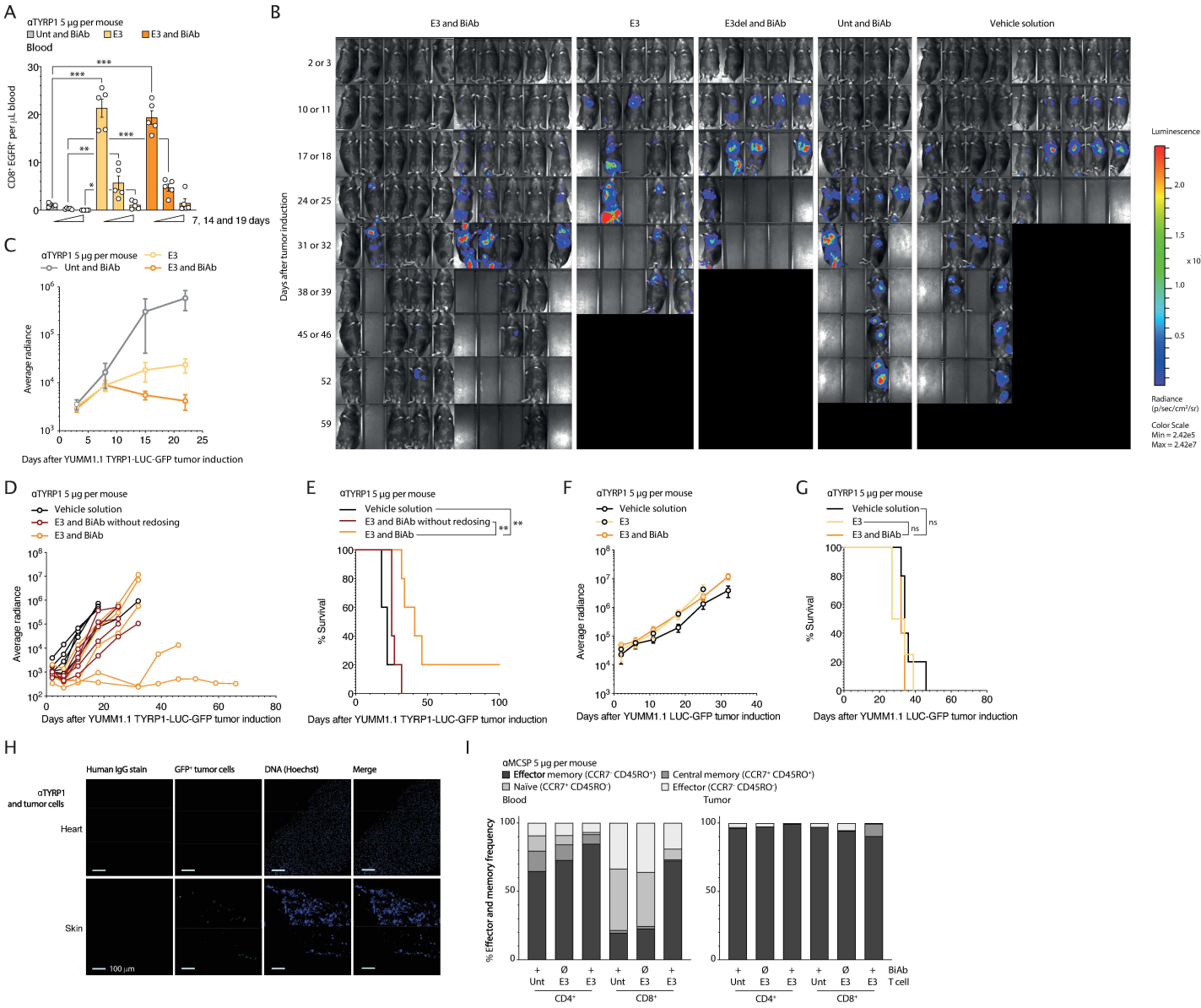
Supplementary figure 2



Supplementary figure 3



Supplementary figure 4



BiAb redirect SAR T cell therapy in melanoma**Supplementary figure 1: MCSP and TYRP1 expression on patient-derived melanoma****samples, human and murine melanoma cell lines, structure and binding properties of** **α TYRP1/ α E3 and α MCSP/ α E3 BiAb.** A) MCSP and TYRP1 protein expression was

assessed with either one of the BiAb (human IgG1) and anti-human IgG secondary antibody.

Median fluorescence intensity (MFI) ratio of MCSP or TYRP1 stain and secondary antibody

only stain was depicted below each flow cytometry plot. B) and C) Schematic drawing of the

α MCSP/ α E3 BiAb molecule in (B) and the α TYRP1/ α E3 in (C). VL and VH, variable domain

of immunoglobulin (Ig) light or heavy chain. CK, constant domain of Ig light chain kappa.

CH1/2/3, first/second/third constant domain of Ig heavy chain. E, R, K, P, G, L, A, amino

acids. D-F) Dissociation constant (K_D) determination of BiAb modules. Binding to MCSP in

(D) ($K_D = 1.1 \mu\text{g/mL}$), TYRP1 in (E) ($K_D = 18 \mu\text{g/mL}$), and EGFRvIII in (F) ($K_D = 42 \text{ ng/mL}$) on

MV3, YUMM1.1 TYRP1 or E3 SAR T cells, as measured by flow cytometry. G) RT-PCR

TYRP1 gene analysis of murine cell lines, and murine T cells. H) TYRP1 protein expression

was assessed with α TYRP1/ α E3 BiAb (human IgG1) and anti-human IgG secondary

antibody. I) Microscopic analysis of TYRP1 expression on permeabilized YUMM1.1,

YUMM1.1 TYRP1, B16 and Panc02-Ova cells using α TYRP1/ α E3 BiAb (α TYRP1) and anti-

human IgG secondary antibody. Experiments show mean values of two biological

experiments for (D), (E) and (F), one experiment for (A), and (H). Experiments in subfigure

(G) show mean values \pm SD calculated from 3 technical replicates and one representative of

two independent experiments in subfigure (I).

Supplementary figure 2: α TYRP1/ α E3 BiAb activates SAR T cells to mediate specific**cytotoxicity against murine melanoma cell lines.** A) ELISA for granzyme B, IFN- γ , IL-2

and TNF- α on supernatant of murine T cells in coculture with murine melanoma cell lines

YUMM1.1 TYRP1 or B16 (E:T 2:1) and α TYRP1/ α E3 BiAb (α TYRP1, 1 $\mu\text{g/mL}$). Supernatant

was taken after 24, 48 and 72 hours (n = 3). B) Frequency of PD-1 and CD69 expression on

27 T cells after 0, 24 and 48 hours of coculture with murine melanoma cell lines YUMM1.1
28 TYRP1, B16 or murine pancreatic cancer cell line Panc02-Ova (E:T 2:1) and α TYRP1/ α E3
29 BiAb (1 μ g/mL) (n = 3). C) Following 48 hours of coculture the CD3⁺ T cell count was
30 assessed using a flow cytometry-based readout and normalized to the 0 hour conditions
31 (n = 3). D) The percentage lysis of melanoma cell lines YUMM1.1 TYRP1, B16 and Panc02-
32 Ova mediated via α TYRP1/ α E3 BiAb and SAR T cells. The cytotoxicity was assessed with a
33 LDH assay after 48 hours of coculture (n = 3). E) ELISA for IFN- γ on supernatant of murine T
34 cells in coculture with murine melanoma cell lines YUMM1.1 TYRP1, B16 or Panc02-Ova
35 (E:T 2:1) and α TYRP1/ α E3 BiAb (α TYRP1, 1 μ g/mL). Statistical analysis was performed
36 using the unpaired two-tailed Student's t test. Statistics shown in (A) were calculated based
37 on the 24 hour time points. Experiments show mean values \pm SD calculated from 3
38 biological replicates and are representative of three independent experiments (A, B, D and
39 E) and mean values \pm SEM calculated from n independent biological replicates (C).

40

41 **Supplementary figure 3: Modular, selective and reversible activation of SAR T cells,**
42 **irrespective of soluble forms of TYRP1 tumor antigen.** A) A375 melanoma cells were
43 plated and cocultured with human SAR T cells (E:T 2:1) and α TYRP1/ α E3 BiAb (α TYRP1, 1
44 μ g/mL). Different concentrations of soluble, recombinant TYRP1 (rTYRP1) were added. The
45 tumor cell lysis over time was assessed using xCELLigence (n = 3). The cell index was
46 normalized to the respective time point of T cell addition as indicated by an arrow. B) Human
47 SAR or E3del control T cells and α TYRP1/ α E3 BiAb (1 μ g/mL) were plated in wells that
48 were either coated with different concentrations of rTYRP1 or where different concentrations
49 of soluble rTYRP1 were added to the medium. After 48 hours the supernatant was taken and
50 analyzed for IFN- γ using ELISA (n = 3). C) Schematic overview of the assay setup from
51 experiments in Figure 4 (D) and (E). Analyses of differences between groups for (A) were
52 performed using two-way ANOVA with correction for multiple testing by the Bonferroni

BiAb redirect SAR T cell therapy in melanoma

53 method. For statistical analysis of (B), the unpaired two-tailed Student's t test was used.

54 Experiments show mean values \pm SD calculated from 3 biological replicates and are

55 representative of three independent experiments.

56

57 **Supplementary figure 4: Treatment with the SAR T cell-BiAb combination is effective**

58 **in syngeneic and xenograft melanoma models.** A) The murine CD8⁺ SAR T cell

59 persistence per μ L blood was analyzed using flow cytometry 7, 14 and 19 days after T cell

60 transfer. The mice were treated according to the experiment in Figure 5 (C). B) *In vivo*

61 imaging data of Figure 5 (A) displaying luminescent signal in radiance for all experimental

62 groups two or three days after YUMM1.1 TYRP1-LUC-GFP tumor induction onwards (days

63 2/3, 10/11, 17/18, 24/25, 31/32, 38/39, 45/46, 52 and 59). C) YUMM1.1 TYRP1-LUC-GFP

64 tumor growth curves of experiment depicted in Figure 5 (C) based on *in vivo* luminescent

65 signal imaging (days 3, 8, 15 and 22). D) YUMM1.1 TYRP1-LUC-GFP tumor growth curves

66 based on *in vivo* luminescent signal imaging (days 2, 6, 11, 18, 25, 32, 39 and 45; for each

67 group n = 5). The mice were treated according to the experiment in Figure 5 (A) with either

68 SAR T cells and α TYRP1/ α E3 BiAb (redosed twice per week), SAR T cells and

69 α TYRP1/ α E3 BiAb (one dose) or the vehicle solution (for all groups: n = 5). E) Percentage

70 survival readout. F) YUMM1.1 LUC-GFP tumor growth curves based on *in vivo* luminescent

71 signal imaging (days 2, 6, 11, 18, 25 and 32). The mice were treated according to the

72 experiment in Figure 5 (A) with either SAR T cells and α TYRP1/ α E3 BiAb (redosed twice per

73 week) (n = 5), SAR T cells (n = 4), or the vehicle solution (n = 5). The experiment was

74 simultaneously conducted with the experiment depicted in Supplementary Figure 4D. G)

75 Percentage survival readout. H) Immunofluorescence imaging of the α TYRP1/ α E3 BiAb and

76 tumor cell-derived GFP in heart and skin tissue of tumor bearing mice injected with the

77 α TYRP1/ α E3 BiAb. The mice were treated according to the experiment in Figure 5 (D). I)

78 Frequency of effector memory (CCR7⁻ and CD45RO⁺), central memory (CCR7⁺ and

79 CD45RO⁺), naïve (CCR7⁺ and CD45RO⁻) and effector (CCR7⁻ and CD45RO⁻) phenotype on
80 human CD4⁺ and CD8⁺ T cells in blood and tumor 14 days after T cell transfer. For statistical
81 analysis of (A), the unpaired two-tailed Student's t test was used. For statistical analysis of
82 survival data, the log-rank test was applied. Experiments show mean values \pm SEM
83 calculated from n biological replicates, one experiment for (A), (D), (E), (F), (G), (H) and (I)
84 and one representative of two independent experiments in (B) and (C).